Fall 12-16-2022

Hydrologic modeling with remote sensing for the estimation of groundwater resources within the Sand River Catchment, South Africa

Sophia Bakar

HYDROLOGICAL MODELING WITH REMOTE SENSING FOR THE ESTIMATION OF GROUNDWATER RESOURCES WITHIN THE SAND RIVER CATCHMENT, SOUTH AFRICA

A Thesis

Submitted to the Bayer School of Natural and Environmental Sciences

Duquesne University

In partial fulfillment of the requirements for

the degree of Master of Science

By

Sophia Bakar

December 2022

HYDROLOGICAL MODELING WITH REMOTE SENSING FOR THE ESTIMATION OF GROUNDWATER RESOURCES WITHIN THE SAND RIVER CATCHMENT, SOUTH AFRICA

By

Sophia Bakar

Approved November 11th, 2022

David M. Kahler Professor of Environmental Science (Committee Chair)	Joshua N. Edokpayi Professor of Environmental Science (Committee Member)
Neil Brown Professor of Environmental Science (Committee Member)	
Ellen Gawalt Dean, Bayer School of Natural and Environmental Sciences	John F. Stolz Director, Center for Environmental Research and Education

ABSTRACT

HYDROLOGICAL MODELING WITH REMOTE SENSING FOR THE ESTIMATION OF GROUNDWATER RESOURCES WITHIN THE SAND RIVER CATCHMENT, SOUTH AFRICA

By

Sophia Bakar

December 2022

Dissertation supervised by Professor David M. Kahler

The Sand River Catchment is an important tributary of the transboundary Limpopo River in South Africa, which spans Botswana, Mozambique, South Africa, and Mozambique. Groundwater is a critical resource in the region, especially in the context of population growth and climate change. Data are needed for proper management of these water resources. In regions where groundwater data are sparse in time, space, or both, the most promising solutions come from satellites and hydrologic models. Regional literature suggests that the Soutpansberg Mountains, located within the Sand Catchment, are high-elevation water towers with uncertain groundwater resources. Improved understanding of groundwater resources in this watershed is critical for water resources management in downstream areas of the Sand River catchment. Groundwater resources in the Soutpansberg Mountains watershed were estimated via a hydrologic modelling and catchment water balance approach and validated with field data using

electrical resistivity tomography. Groundwater data were obtained from NASA's Gravity Recovery and Climate Experiment (GRACE). Precipitation and surface water data were obtained from the South Africa Department of Water and Sanitation (DWS) gage network. Additional data for surface water components were obtained from the Global Land Data Assimilation System (GLDAS) that combines satellite and ground-based data with land surface models and data assimilation. Flow and infiltration were modelled using HEC-HMS (U.S. Army Corps of Engineers). The model and water balance results support the hypothesis that the Soutpansberg Mountains watershed is a high recharge area that requires monitoring for sustainable use.

ACKNOWLEDGMENTS

I would like to thank my advisor Dr. David M. Kahler, professor and committee member Dr. Joshua Edokpayi, professor and committee member Dr. Neil Brown, the United States Agency for International Development (USAID), members and stakeholders of the Water Q2 Project, lab member Gabriella Zuccolotto, lab member Jake Agate, and the Center for Environmental Research and Education at Duquesne University for the support, resources, funding, and opportunities related to this research. This work was financially supported by USAID- Southern African Regional Development Mission Award 72067419FA00001. This work does not necessarily reflect the views of USAID or the United States Government.

TABLE OF CONTENTS

LIST OF TABLES

LIST OF FIGURES

LIST OF ACRONYMS

Limpopo River Basin – LRB

Integrated Water Resources Management - IWRM

Limpopo Watercourse Commission – LIMCOM

Southern African Development Community – SADC

SADC Groundwater Management Institute – SADC-GMI

LIMCOM Groundwater Committee – LGC

South Africa Department of Water and Sanitation – DWS

Evapotranspiration - ET

National Aeronautics and Space Administration - NASA

Gravity Recovery and Climate Experiment – GRACE

Global Land Data Assimilation System – GLDAS

Digital Elevation Model – DEM

Shuttle Radar Topography Mission – SRTM

Moderate Resolution Imaging Spectroradiometer - MODIS

Soil Moisture – SM

Snowmelt – SWE

Canopy Water Storage – CA

Terrestrial Water Storage – TWS

Costal Resolution Improvement – CRI

Jet Propulsion Laboratory - JPL

Surface Water – SW

CHAPTER 1: INTRODUCTION

Groundwater serves as a primary source of freshwater for drinking and irrigation purposes for approximately 2.5 billion people globally (Ahmed, 2020; Bhanja & Mukherjee, 2019; Li et al., 2019; Rodell et al., 2009). Groundwater resources are particularly important at transboundary aquifer sites, where political and aquifer boundaries overlap, and in arid and semi-arid regions, where rivers and lakes are sustained by groundwater discharge (Abiye & Leketa, 2021). In low-and-middle income countries (LMIC), especially those in arid and semi-arid regions, groundwater resources play a critical role in supplying water to support growing populations and for a range of economic sectors including agriculture, urban development, industrial uses, and mining (Abiye & Leketa, 2021; Petrie et al., 2014). Sustainability of groundwater in these regions is threatened by depletion due to increased use, deteriorated water quality, and climate changes that alter aquifer recharge rates (Rohde et al., 2020). Overuse of these resources can lead to a reduction of regional agricultural output and shortages of potable water, causing extensive socio-economic stresses (Abiye & Leketa, 2021; Li et al., 2019). To ensure successful community planning, improved economic development, and resource protection, there is a need for improved water resources management practices and appropriate groundwater threshold recommendations, especially in countries that share aquifer resources (IGRAC, 2020). These must be supported by accurate hydrologic data and holistic groundwater assessments (Li et al., 2019; Mosase, 2018; Neves et al., 2020; Rodell & Famiglietti, 2001; Tapley et al., 2019). This study utilizes hydrologic modeling and a catchment water balance approach to assess groundwater resources in the Sand River Catchment of the arid/semi-arid and transboundary Limpopo River Basin (LRB).

1.1 The Limpopo River Basin

The Limpopo River Basin (LRB) is shared by Botswana, Mozambique, South Africa, and Zimbabwe and covers 416, 296 km^2 (Table 1). The majority of the basin lies in South Africa, where the river flows north, forms the border between South Africa and Botswana, the border between South Africa and Zimbabwe, and then through Mozambique into the Indian Ocean, traveling a length of 1,770 km (Figure 1). The water resources within the basin support approximately 18 million people and biodiversity (Earle, 2006; RESILIM, 2017; Saveca et al., 2022; Walker et al., 2018). Biodiversity hotspots include Kruger National Park in South Africa, Limpopo National Park in Mozambique, the Gonarezhou National Park in Zimbabwe, and numerous other parks and UNESCO sites (Global Environment Facility, 2019).

Table 1.Population and area of the countries in the LRB (RESILIM, 2017).

Country	Area of LRB (km^2)	Percentage of LRB	Population in LRB	Total Population
South Africa	187,333	45%	15,078,510 (25%)	59.3 million
Mozambique	87,422	20%	1,109,481 (4%)	31.3 million
Botswana	79,096	20%	1,197,314 (37%)	3.2 million
Zimbabwe	62,444	15%	831,747 (5%)	14.8 million

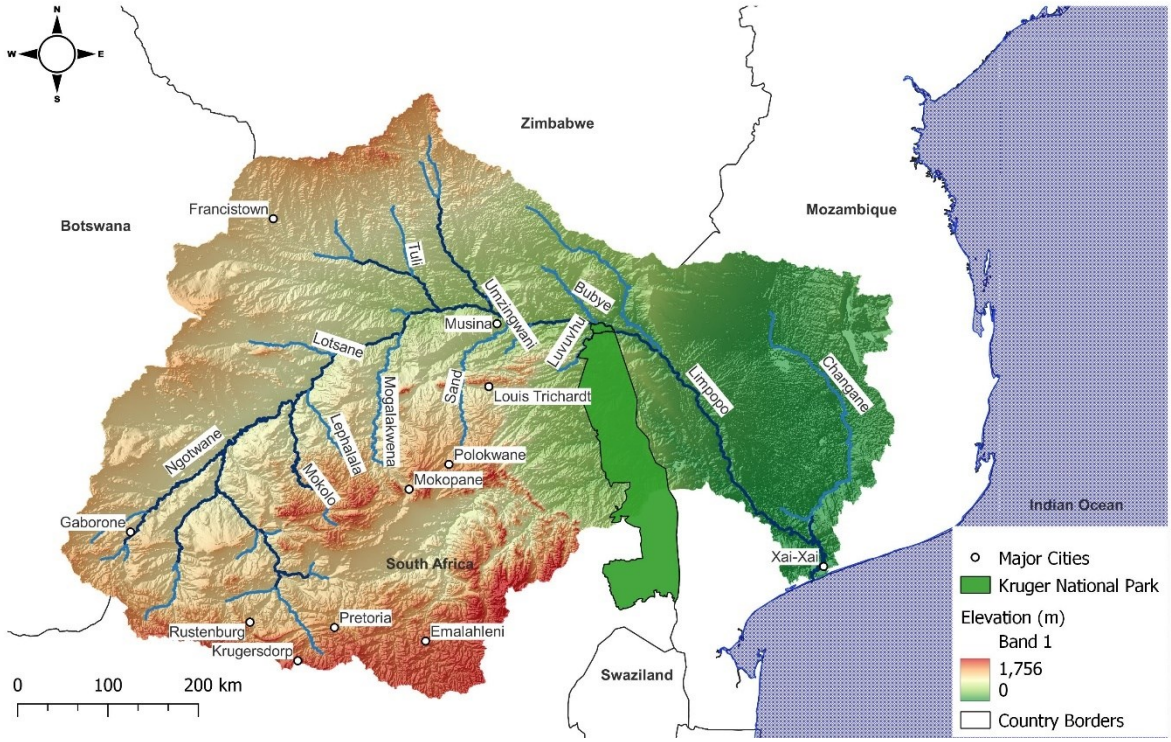

Figure 1. Geography of the Limpopo River Basin, including elevation generated from SRTM Digital Elevation Model (NASA JPL, 2013) *and, African country and Limpopo River shapefiles* (Martin, 2021).

Economic activities, which vary significantly across the riparian countries, include livestock farming, agriculture, mining, light industries, tourism, and fishing (Earle et al., 2005; Earle, 2006; Environmentek-CSIR, 2003; RESILIM, 2017). Each of these requires water as an essential resource. Availability of water resources in the basin varies due to interannual climate variability, occurrence of severe floods and droughts, industrial water demand, and domestic water demand. The basin's water resources are increasingly stressed due to population growth, increasing industrial development, agricultural activities, and climate change impacts. The combination of these presents unique challenges for the future management of water resources in the basin (Bhanja & Mukherjee, 2019; Mosase, 2018; Nicholson et al., 2013; Rohde et al., 2020).

1.1.1 Climate and Topography

The climate of the LRB is tropical/sub-tropical dry savannah and is controlled by the basin's position in a continental, equatorial convergence zone and the presence of subtropical eastern and marine western Mediterranean air masses (Botai et al., 2020; Global Environment Facility, 2019). Water resources in the basin are affected by extreme seasonality, El Niño-Southern Oscillation (ENSO) events, and coastal interactions. Approximately 95% of rainfall occurs between October and April and is spatially and temporally heterogeneous. Hot, dry areas may receive as little as 200 mm precipitation annually, while high rainfall areas may receive up to 1500 mm annually (Environmentek-CSIR, 2003; RESILIM, 2017). The mean annual precipitation across the basin is 530 mm/year(Limpopo Basin Permanent Technical Committee, 2010). Evapotranspiration rates across the basin range from 400 mm/year to 1100 mm/year (Alemaw, 2012). The unreliability of rainfall and runoff throughout the basin contributes to the occurrence of floods and droughts (Botai et al., 2020; Mosase, 2018). The frequency of these extreme hydrological events is also associated with temperature increase induced by climate change (Botai et al., 2020; Environmentek-CSIR, 2003; Nicholson et al., 2013; Petrie et al., 2014).

The topography of the basin also varies considerably. The basin is generally divided into two plateau areas. The upland plateau is formed by the area of the LRB shared by Botswana, South Africa and Zimbabwe in the north and bordered by the Waterberg, Strydpoort, and Drakensberg Mountains in the south. The highest elevations in the basin, greater than 2,000 meters, occur within this stretch of mountains (Figure 1). This plateau is characterized by deeply incised (up to 600 meters) river valleys (Chinoda et al., 2009; CPWF, 2014). The lowland, coastal plateau contains the area of the LRB located in north-east South Africa, south-east

Zimbabwe, and southern Mozambique. This plateau is flatter and contains broad, low-lying valleys. The lowest elevations occur in the floodplains of southern Mozambique, where the river reaches the ocean; the lowest point is at sea level.

1.1.2 Water Supply and Demand

The annual variability in rainfall and runoff presents challenges for developing regional water budgets across the LRB. Distribution of water is of strategic importance to support increasing social and economic development. Current water uses and demand across the LRB reflect the significance of agriculture, urban development, and mining in the region. Total water demand is 4,459 million m^3/year (Table 2), with only approximately 4,000 million m^3/year available via runoff (Global Environment Facility, 2019).The demand deficit is met by extracting groundwater, which is generally used to support irrigation (Earle, 2006; RESILIM, 2017). Agriculture is the predominant activity for water use in all four riparian countries and is the sector with the greatest water requirement (Table 2) (Global Environment Facility, 2019; Tapela & Massingue, 2010). The domestic water demand supports household use, livestock watering, and small-farm irrigation in rural communities and for urban supply in major cities.

Table 2. LRB water demand by country and sector (CSIR 2003, Ramoeli 2010, GEF 2019)

Water Requirements, (million m^3/year)	Botswana	Mozambique	South Africa	Zimbabwe	Total
Domestic	53	32	901	86	1072 (24%)
Industrial	0	n/a	327	1	328 (7%)
Mining	8	n/a	285	6	299 (7%)
Irrigation	7	274	1974	96	2351 (53%)
Forestry	n/a	n/a	83	n/a	83 (2%)
Livestock	20	21	45	14	100 (2%)

Thermal Electric	3	n/a	223	n/a	226 (5%)
Total	91 (2%)	327 (7%)	3838 (86%)	203 (5%)	4459

The LRB is considered "closed" in terms of water management (RESILIM, 2017). This means that the current demand exceeds the amount of surface water available annually. Additionally, there has been an observed decline in surface water resources as a result of rapid urban population growth, expansion of mining and energy projects, and large-scale national development projects (Chinoda et al., 2009; Environmentek-CSIR, 2003; RESILIM, 2017). Surface water availability is also heavily impacted by the presence of dams along the river and the diversion of streamflow for irrigation (Petrie et al., 2014). Reductions in streamflow result in a reduction of water supply for downstream ecosystems, increased sedimentation at reservoir sites and reduction of water storage capacity, loss of biodiversity, and increased saltwater intrusion at coastal areas (CPWF, 2014; Global Environment Facility, 2019). Despite an existing decline in available water resources (Mosase, 2018; RESILIM, 2017), water demand in the basin is expected to increase, by as much as 46% by 2025 (Petrie et al., 2014; Tapela & Massingue, 2010). Under these conditions, water scarcity is likely and will be further exacerbated by land degradation, pollution, and climate-change related impacts (Chinoda et al., 2009; Environmentek-CSIR, 2003). Water scarcity occurs when water demand exceeds availability and is the greatest threat to the livelihood, economy, and environment of the region. The socio-economic impacts of water supply issues include the persistence of poverty, food-insecurity, and water insecurity facing communities across the basin (Botai et al., 2020).

1.1.3 Water Resources Management

Water governance in transboundary river basins is complex and can potentially lead to conflict among riparian states. Collaboration between the LRB countries and effective

management strategies reduces regional conflict and promotes sufficient access to clean water to meet all sector demands across the basin. In the past 20 years, transboundary water governance and regional non-profits have been established to address critical issues related to water resources monitoring, data, sharing, and management within the LRB. In 2003, the Limpopo Watercourse Commission (LIMCOM) was established between the riparian countries as an entity to focus on shared international water issues and provide recommendations on the uses of the water resources of the LRB (The Limpopo Watercourse Commission (LIMCOM), 2003). This cooperation did not explicitly include groundwater resources management, as generally there is an institutional separation of groundwater and surface water resources. In 2018, the Southern Africa Development Community (SADC) Groundwater Management Institute (SADC-GMI) and LIMCOM signed a Memorandum of Understanding (MoU) for collaboration on groundwater issues in the LRB (SADC-GMI, 2020). In 2019, a formal cooperation mechanism was established to focus on groundwater resources and management. The collaboration between these organizations covers:

- Transboundary cooperation to integrate groundwater resources between the riparian countries
- Support of international data sharing and solutions to address shared groundwater challenges
- The promotion of transboundary aquifer management in collaboration with relevant governing authorities
- Research on groundwater challenges involving studies, information exchange, and training and implantation of solutions

- Information and technologies for creating a shared platform to build an integrated data management system

The LIMCOM Groundwater Committee (LGC), established as a result of this collaboration, is now officially the institutional structure recognized by regional entities to drive groundwater resources management in the LRB. Limitations and challenges recognized by the LGC include lack of data sharing and availability, lack of groundwater monitoring structure, institutional challenges related to collaboration with international entities, and a knowledge gap between upstream and downstream interactions (Tapela & Massingue, 2010).

SADC, established in 1992, is a regional economic community of 16 member states: Angola, Botswana, Comoros, Democratic Republic of Congo, Eswatini, Madagascar, Malawi, Mauritius, Mozambique, Namibia, Seychelles, South Africa, Tanzania, Zambia, and Zimbabwe. The community is dedicated to regional integration and poverty eradication through economic development. In the southern African region, approximately 70% of the population experiences negative socio-economic impacts because of water supply issues (Botai et al., 2020; SADC, 2022). In 2008, SADC-GMI was established in recognition of the importance of groundwater resources for regional water security, strengthening livelihoods, enhancing economic growth, and reducing vulnerability to climate change (SADC, 2022; SADC-GMI, 2020). SADC-GMI's main objectives are to promote sustainable groundwater resources management and provide solutions to groundwater challenges across the SADC region. The organization works to support this objective through a groundwater data resource center and information portal (SADC-GMI, 2010b), annual report and financial sustainability plans (SADC-GMI, 2020), and projects that support capacity building, knowledge development, and inclusivity in groundwater management (SADC-GMI, 2021).

1.2 Study Area: The Sand River Catchment

1.2.1 Ephemeral Rivers

Approximately 2 billion people globally live in drylands and obtain their water supply from ephemeral rivers (Walker et al., 2018). Ephemeral, sand choked rivers commonly appear in the world's dryland regions, where surface flows only occur following infrequent, torrential rainfall (Walker et al., 2018). Surface flow through ephemeral rivers will only occur when the alluvial basal sands are fully saturated (Love et al., 2008; Walker et al., 2018). As water accumulates within saturated basal sands, limited aquifers are formed. Long-term depletion of these resources is not expected as the frequency of surface water flow equates to the recharge frequency of the aquifer (Walker et al., 2018, 2019). The frequent recharge and consistent availability of water resources in ephemeral river catchments are particularly useful to fulfill the domestic and small-scale agriculture demand of poor, rural communities.

1.2.2 The Sand River Catchment and Soutpansberg Mountains

The Sand River is an important ephemeral tributary of the Limpopo River in South Africa (Figure 2). It flows into the Limpopo near both the border of South Africa and Zimbabwe and the border of South Africa and Botswana. The catchment covers 15,777 km^2, which represents 8% of the area of the LRB in South Africa and 3% of the total basin area (Table 1). In lower elevation areas of the catchment, little to no observed surface water flow occurs (Walker et al., 2018). Significant surface water flows in the catchment are observed in the streams from the Soutpansberg Mountains, where high-intensity rainfall and steep slopes cause major tributaries to flow above the bedrock and encourage runoff (Environmentek-CSIR, 2003; Walker et al., 2018). The elevation and forested nature of the Soutpansberg mountains contributes important hydrological function to overall surface and groundwater interactions within the catchment by

moderating streamflow and maintaining a high infiltration rate (Petrie et al., 2014). The annual runoff observed from the Soutpansberg mountains may be up to 100 times that of the lower-lying areas of the catchment.

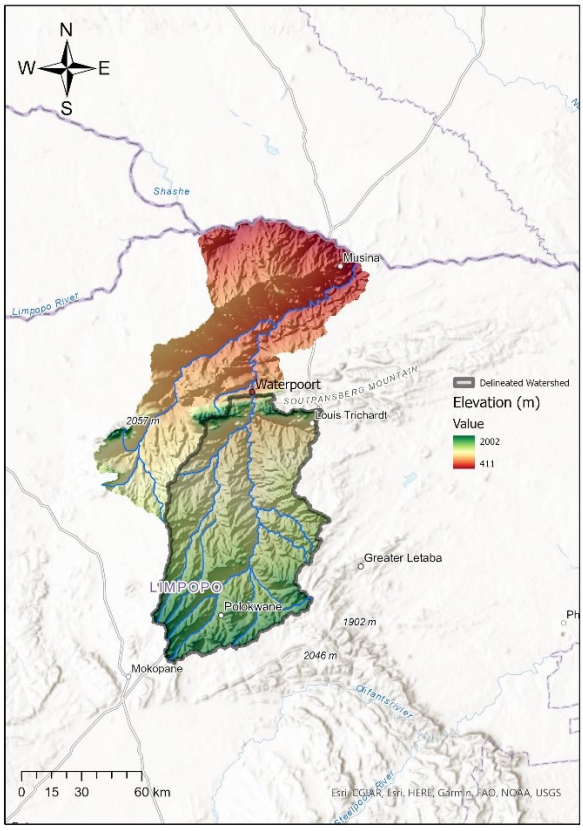

Figure 2. Geography of the Sand River Catchment, including elevation (NASA JPL, 2013) *and, river and catchment shapefiles* (Martin, 2021).

The surface and ground water resources of the Soutpansberg Mountains are essential to local farming, mining, domestic water supply, and regional development. There are more than 700 small farms that utilize stock watering and intensive irrigation, almost exclusively from groundwater resources extracted from the saturated alluvium aquifer that feeds the tributaries and baseflow of the Sand River (Environmentek-CSIR, 2003). The Sand River catchment, specifically the area within the Soutpansberg mountains, is also a center of endism and biodiversity (van Wyck & Smith, 2001). Between 2,500 and 3,000 indigenous plant species grow in the mountains, representing approximately 68% of all plant families native to the southern

African region. Additionally, the Soutpansberg is known for high avian diversity and home to species under threat at a global level. The hydrological ecosystem services provided by the Sand River watershed within the Soutpansberg Mountains are crucial to maintaining regional resilience. Understanding the frequency of flow and recharge in this watershed of the Sand River catchment is necessary for effectively managing groundwater resources to support the regional population, increased development in upstream areas of the catchment, and protect vulnerable biodiversity.

1.2.3 Regional Groundwater Resources Management

In South Africa, there are two datasets providing the standard for groundwater resources management, active monitoring boreholes installed and managed by the South Africa Department of Water and Sanitation (DWS) and borehole information from SADC-GMI. The data from the monitoring boreholes managed by DWS have temporal and spatial limitations in the Limpopo Province. The data from each borehole are not necessarily available over the same

time period. Data from all the monitoring boreholes in the Limpopo Province were obtained, but there are no active monitoring sites in the Sand River Catchment (Figure 3).

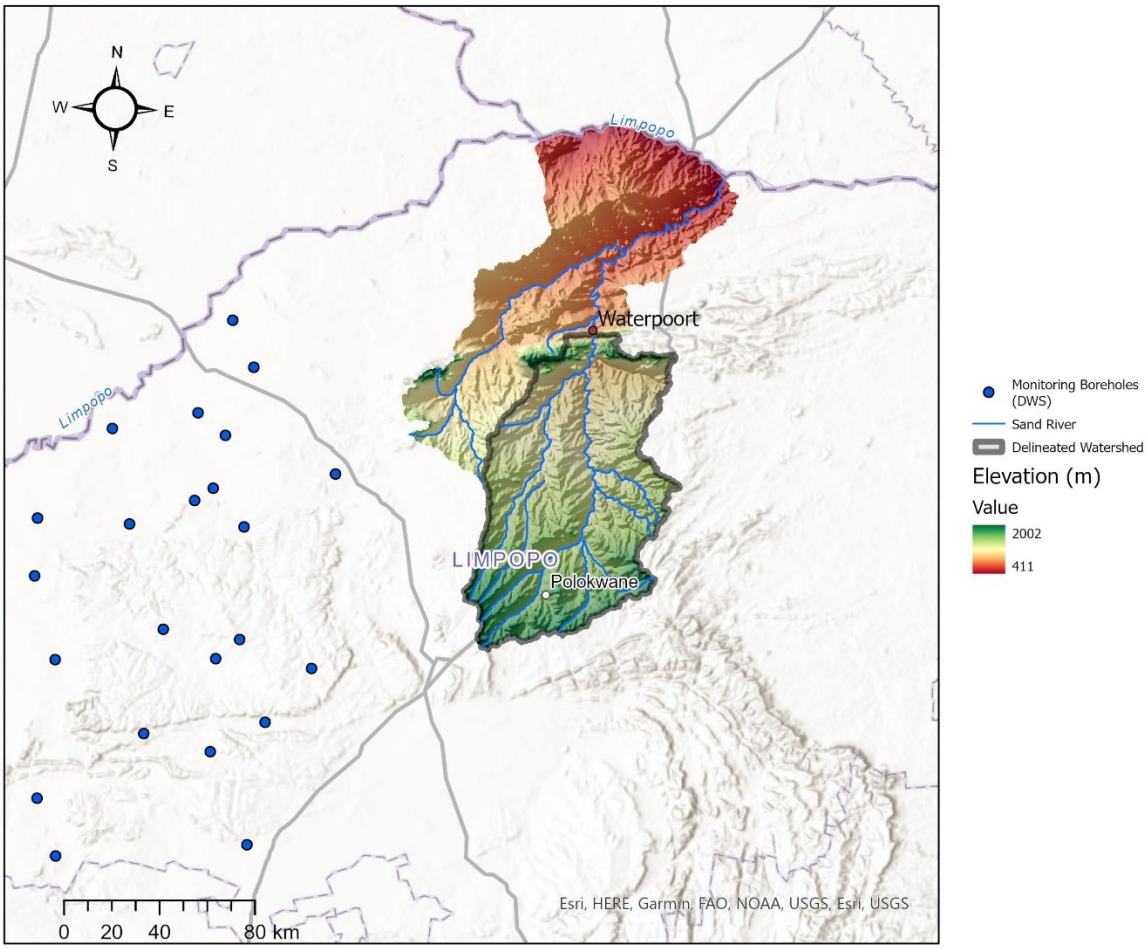

Figure 3. Active monitoring boreholes established by DWS in the Limpopo Province (Department of Water and Sanitation, 2011).

SADC-GMI is working to improve knowledge and management of groundwater resources via a hydrogeological mapping project and atlas intended to provide information on the extent and geometry of regional aquifer systems (Ramoeli et al., 2010). This project produced a borehole database in 2010 with the available drilling records for each riparian country, which have been used as a standard for understanding groundwater use in the LRB. This project represents a regional effort to collaborate and disseminate data for improved transboundary

groundwater management but has several limitations. The dataset is static and available only until 2010. The required inputs for each borehole do not have a measurement standard and therefore varies greatly from borehole to borehole. Additionally, there is minimal information on how or by whom the data were collected, and quality control measures taken. However, the aggregate data may be useful for observing the depth of the water table over time and providing information about the regional aquifer types. The lack of groundwater monitoring data from DWS in this catchment and the limitations of the SADC-GMI dataset present a need for improved groundwater data collection and monitoring.

1.3 Objectives and Motivation

High quality, historical meteorological datasets are often limited or unavailable in LMIC; this is true of the countries in the LRB (Earle, 2006; Environmentek-CSIR, 2003; Walker et al., 2018, 2019). These data are necessary for hydrologic modelling purposes and improved water resources management. This study aims to fill groundwater data gaps and show that the Soutpansberg Mountains in the Sand River Catchment act as high elevation water towers. This is accomplished by assessing infiltration and monthly changes in groundwater levels via a catchment water balance, modeling flow and infiltration, and validating these results with in-situ electrical resistivity tomography (ERT) measurements. The combination of these methods demonstrates the unique capability and benefits of using remotely sensed, modelled, and in-situ data for improved water resources management in a data-scarce region. The results of the study support regional governance objectives by building the capacity of stakeholders to sustainably manage groundwater resources and a high-priority ecosystem (RESILIM, 2017; Tapela & Massingue, 2010). The region faces threats to water security including increasing population, pollution, land degradation, climate change impacts, and increased agriculture demand.

Groundwater resources monitoring and management play a critical role in mitigating the impacts of these threats and supporting increased development. To our knowledge, this the first groundwater resources assessment of the Sand River catchment at the Soutpansberg Mountains.

CHAPTER 2: DATA

2.1 Ground-Based Measurements and Derived Data

2.1.1 SADC-GMI Borehole Data

Borehole information from 438 boreholes from the period 2000-2010 in and surrounding the Sand River Catchment were obtained (Figure 4) (SADC-GMI, 2010a). Elevation, borehole depth, date of drilling, and aquifer characteristic data for each borehole were collected. Drilling depth for each borehole was determined by subtracting the borehole depth from the elevation (Figure 9).

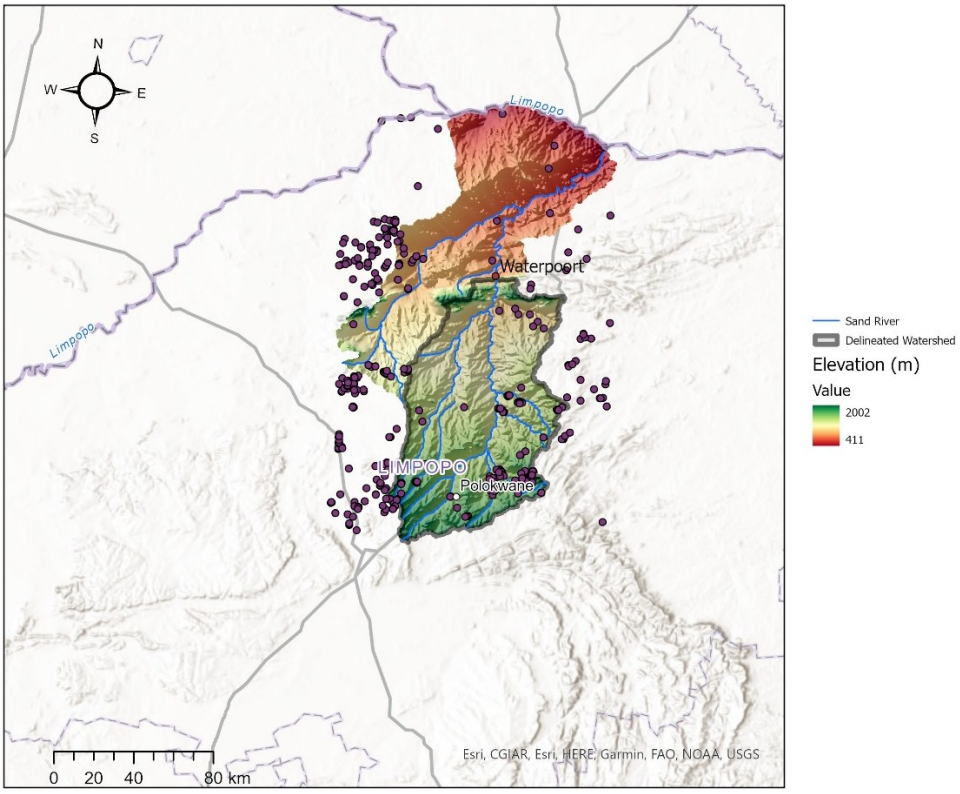

Figure 4. SADC-GMI boreholes in the Sand River Catchment (SADC-GMI, 2010a).

2.1.2 In-Situ Hydrometeorological Measurements

DWS maintains a network of river gages and weather stations (Department of Water and Sanitation, 2011). River flow data from the Sand River at Waterpoort was used to provide comparison and validation for model results (Figure 5).

Figure 5. Weir at Waterpoort, used as outlet point for delineated watershed and developed model.

Precipitation data for this research included data from 32 gages in both the Limpopo and Olifants drainage regions. The data collected were from August 2009 to July 2020. Data were averaged via the Thiessen Method for areal rainfall. The Thiessen Method uses polygons to calculate areas in relation to specific rain gages and then computer the average amount of precipitation that fell in a specific basin or area (Chow et al., 1988).

The Water Q2 Project installed four hydrometeorological stations at the Mutale Weir, Mbahela Primary School on the Mutale River, the Medike Nature Reserve on the Sand River, and Leshiba Wetland on an unnamed tributary of the Sand River (Kahler et al., 2019). This research utilizes data from the Medike Nature Reserve station, which was installed August 2019 and measures 15-minute precipitation, solar radiation, air temperature, relative humidity, and

wind speed and direction. All data are outputs from the instruments except relative humidity, which is the ratio of the actual vapor pressure and its saturation at a given air temperature (Chow et al., 1988).

Precipitation is measured with an electronic drip-counter rain gage (ATMOS41, Meter Group, Pullman, WA, USA). Data are recorded via cloud-based Zl6 (Meter Group) cellular-enabled data logger and transmitted every hour. These data are publicly available (Kahler, 2020).

2.1.2 Estimated Evapotranspiration

The advection-aridity evapotranspiration model generated by Brutsaert and Stricker (1979) is based on a complimentary approach to the model developed by Bouchet 1963, where the excess in potential evaporation (PE) is equal to the deficit in actual evapotranspiration (ET), and aridity is deduced from large-scale advection of the drying power of wind (Allen et al., 1998; Bouchet, 1963; Brutsaert & Stricker, 1979). The data required are the same as other well-known combination approaches, such as Penman's equation (Penman, 1948) or the Priestley and Taylor method (Priestley & Taylor, 1972). The main advantage of this model is the use of meteorological parameters only; there is no requirement of soil moisture data, active vegetation moisture, or any other measures of aridity. The equation's general form is:

$$E = A\frac{\Delta}{\Delta+\gamma}(R_n - G) - \frac{\gamma}{\Delta+\gamma}(B + CU_a)(e_a^* - e_a) \qquad (1)$$

where A, B, and B are constants, evaporation (E), net radiation (R_n), and ground heat flux (G) are in mm/d, average wind speed (U_a) is in m/s, and saturation vapor pressure (e_a^*) and vapor pressure (e_a) are in mm Hg. The values of the constants assume the value $\alpha = 1.28$, from

Priestley and Taylor's original formula and are derived from Penman's wind function, where A= 2α - 1 = 1.56, B = 0.35, and C = 0.189. Net radiation and ground heat flux are provided in terms of depth obtained with the latent heat of vaporization and density of water (Chow et al., 1988). This approach has been shown to effectively model evapotranspiration in arid and semi-arid regions (Brutsaert & Stricker, 1979). The data for these calculations were obtained from the weather monitoring site at the Soutpansberg Mountains and used to calculated ET estimates from August 2019 to July 2021.

2.2 Remote Sensing Measurements

Ideally, inputs to hydrologic models are based on in-situ measurements; however, these data may be lacking, costly, and time-consuming (Jiang et al., 2014; Rodell & Famiglietti, 2001). Remote sensing observations offer a useful, low-cost complement to field observations and hydrologic models (Ahmed, 2020; Rzepecka & Birylo, 2020a). This study used a variety of remote sensing measurements (Table 3) to observe trends in terrestrial water storage, provide inputs for the hydrologic model at the Soutpansberg Mountains, and support catchment water balance calculations.

Table 3. Remote sensing measurements used in this study, obtained from August 2009 to July 2019.

Source	Data Product	Units/Format	Resolution
NASA's Gravity Recovery and Climate Experiment (GRACE)	Terrestrial Water Storage (TWS)	mm	0.5˚ x 0.5 ˚
Global Land Data Assimilation System (GLDAS)	Plant Canopy Storage	kg/m^2	0.25 ˚
GLDAS	Soil Moisture	kg/m^2	0.25 ˚
Shuttle Radar Topography Mission (SRTM)	Digital Elevation (DEMs)	Raster/Image	1 arc-second, ~ 30 m

Sentinel-2	Land Cover	Raster/Image	20 m
Moderate Resolution Imaging Spectroradiometer (MODIS)	Evapotranspiration	mm/ 8 days	500 m

2.2.1 GRACE and GRACE-FO Measurements

NASA's Gravity Recovery and Climate Experiment (GRACE) operated from 2002 to 2017 and is succeeded by the GRACE Follow-on mission (GRACE-FO) (Landerer et al., 2020; Watkins et al., 2015; Wiese et al., 2016). These missions are a system of two satellites which fly in identical orbits at approximately 250 km separation distance and measure gravitational anomalies. The measured gravitational anomalies directly correspond to mass changes on the Earth's surface, according to Newton's law of universal gravitation ((Rzepecka & Birylo, 2020b; Watkins et al., 2015). These anomalies are measured in relation to an average baseline value obtained from January 2004 to December 2009. The largest signals observed by GRACE come from spatial and temporal variations in terrestrial water storage (TWS), which is the sum of soil moisture, groundwater, surface waters, snow and ice, canopy interception, and wet biomass (Ahmed et al., 2016; Chanu et al., 2020; Li et al., 2019; Rodell & Famiglietti, 2001). GRACE TWS measurements are limited in that they have low horizontal resolution, and no vertical resolution; the satellites cannot distinguish anomalies resulting from the various TWS components (Ahmed et al., 2016; Chanu et al., 2020). Despite these limitations, GRACE TWS data provide a practical solution to investigate groundwater resources where in-situ data and monitoring are lacking (Ahmed, 2020; Ahmed et al., 2016; Chanu et al., 2020; Frappart & Ramillien, 2018; Rodell & Famiglietti, 2001; Rzepecka & Birylo, 2020b). Groundwater storage estimates can be isolated from GRACE TWS data given information on the other components of

TWS from ground-based observations or data from land surface models (Frappart & Ramillien, 2018; Jiang et al., 2014; Rzepecka & Birylo, 2020b).

GRACE TWS data for the study area was obtained from NASA's Jet Propulsion Laboratory (JPL) in the form of monthly gravity mascon solutions with a coastal resolution improvement (CRI) applied for August 2009 to July 2019 (Landerer, 2021; Landerer & Swenson, 2012). A mascon is a regional mass concentration block with constraints applied during the inversion of the satellite ranging observations (as opposed to after inversion) to better preserve GRACE signals (Watkins et al., 2015; Wiese et al., 2016). NASA JPL's GRACE TWS mascon solutions are derived from 4551 equal area, 3 arc-degree concentration units. Changes in any given mascon capture gravitational variations at each localized cell. The Sand River Catchment lies within the bounds of three JPL mascons. GRACE TWS estimates for the catchment were calculated as the average of the three mascon solutions. Some GRACE TWS monthly data are missing, where data may be excluded due to instrument issues, calibration campaigns, and GRACE battery management (Cooley et al., 2020; NASA JPL, 2022). Missing values were filled with a linear interpolation.

2.2.2 GLDAS Data Products

To derive groundwater storage from GRACE TWS data, remotely sensed estimates of TWS components were obtained from the Global Land Data Assimilation System (GLDAS) (Beaudoing & Rodell, 2020; Landerer, 2021). GLDAS combines satellite and ground-based observational data via land surface modeling and data assimilation techniques to generate land surface states and fluxes to support weather and climate predictions. Data assimilation merges measurements with model predictions, with the goal of maximizing spatial and temporal coverage, consistency, resolution, and accuracy (Rodell et al., 2004). Model observations may be

highly accurate at specific points in space and time, but they are subject to instrument failures, measurement drift, data stream interruptions, missing validation data, and flaws in the algorithms used to derive desired quantities from measured signals (Ahmed, 2020; Rodell et al., 2004). GLDAS provides data assimilation models for terrestrial and energy storages by incorporating model predictions and measurements from land surface, soil, slope and elevation parameters, and ground-based meteorological datasets. GLDAS required forcing fields include precipitation, short and longwave radiation, air temperature, specific humidity, wind speed and direction, and surfaced pressure (Rodell et al., 2004). GLDAS data are available from four sub-models, National Centers for Environmental Prediction/Oregon State University/Air Force/Hydrological Research Lab Model (NOAH), Community Land Surface models (CLM), Variable Infiltration Capacity (VIC), and Mosaic (Beaudoing & Rui, 2021; Rodell et al., 2004)). TWS components from the NOAH model have been successfully used to derive monthly groundwater storage changes from GRACE TWS estimates (Ahmed, 2020; Bhanja & Mukherjee, 2019; Li et al., 2019; Purdy et al., 2019; Rzepecka & Birylo, 2020b).

This study utilized monthly soil moisture and plant canopy storage estimates from the NOAH model with a resolution of 0.25˚ to represent the total amount of water contained in the surface of the Sand River Catchment from August 2009 to July 2020 (Beaudoing & Rodell, 2020; Mocko, 2012; Xia et al., 2012). Snow melt is an additional component of terrestrial water storage but was not considered in this study as there is no snowfall in the study region. Both datasets incorporate soil-vegetation-atmosphere transfer schemes so that the fluxes and storages of energy and water at the land surface are closely related to vegetation properties (Rodell et al., 2004). Soil moisture is modeled to the depth of 2 meters and is estimated based on GLDAS required forcing fields, land cover, and soil texture datasets. Land cover in the NOAH model is

derived from a static 1-km resolution dataset based on observations from the NOAA-15 satellite. Soil texture for the NOAH model is derived from a global hybrid State Soil Geographic Database (STATSGO) and Food and Agriculture Organization (FAO) map produced by the National Center for Atmospheric Research (NCAR) (Pennsylvania State University (PSU), 2006). Plant canopy storage estimates are derived from land cover data and 16-km resolution time series of leaf area index, adjusted for fractional vegetation cover (Rodell et al., 2004). Both data sets are expressed in kg/m^2, which were converted to the equivalent water height in meters by dividing the values by the density of water.

2.2.3 SRTM Digital Elevation Models

A digital elevation model (DEM) is a model of Earth's surface which may be generated using Radar, LiDAR, stereo photogrammetry, and topographic maps. Terrain parameters may be extracted from DEMS and have important applications in geomorphology and modelling water flows (Fathy et al., 2019). DEMs are available from various open sources at different resolutions, but the Shuttle Radar Topography Mission (SRTM) DEM 1-arc second images have been shown to be the most accurate for catchment delineation purposes on a global scale (Fathy et al., 2019). For this research, SRTM DEM 1-arc second global images were obtained over the area of the Sand River Catchment (NASA JPL, 2013). These images are in raster format (e.g. GEOTIFF) and were used in model development by providing terrain information about the region for watershed delineation purposes.

2.2.4 Land Cover

Land cover and land use data are used to model water infiltration into the soil, energy budgets, evaporation, water routing, and sediment flow. Linking land-cover models with hydrologic modelling frameworks allows for the planned management of water resources allows

for the planned management of water resources and facilitates analysis of future vulnerabilities. This study uses 2020 land cover and land use data obtained from the South Africa Department of Forestry, Fisheries, and the Environment (Figure 5) (Department of Forestry Fisheries and the Environment, 2018).

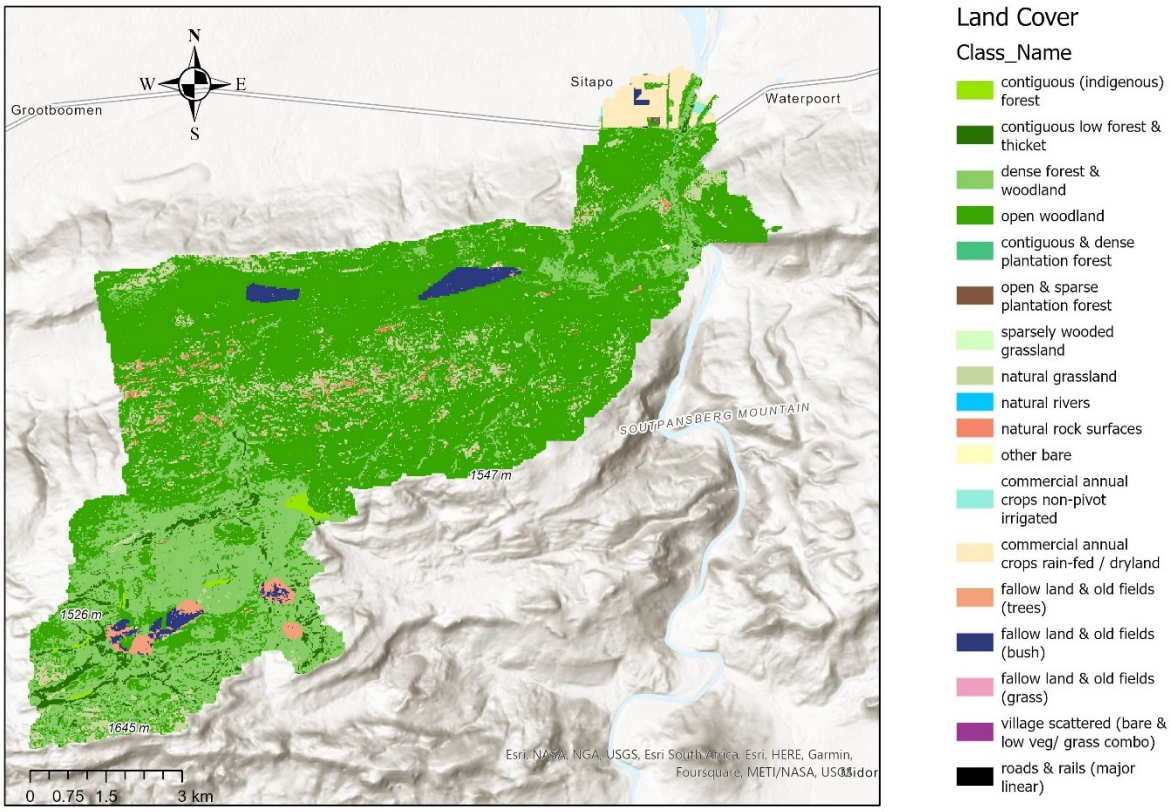

Figure 6. Land cover at the Soutpansberg Mountains (Department of Forestry Fisheries and the Environment, 2018).

The initial datasets were generated from 20-meter, multi-seasonal Sentinel 2 satellite imagery data in 2018. The imagery used represents a full temporal range from January 2018 to December 2018. The 2020 dataset was developed by the Department of Forestry, Fisheries, and the Environment using a computer-automated land cover system that can create automated land-cover datasets, accuracy assessments, and change detection between comparable datasets (Department of Forestry Fisheries and the Environment, 2018).

2.2.5 MODIS Evapotranspiration

NASA's Moderate Resolution Imaging Spectroradiometer (MODIS) provides data products for terrestrial ecosystem evapotranspiration (ET) and potential evapotranspiration (PET) at 500 m spatial resolution, 8-day temporal resolution (Running et al., 2022). The algorithm for ET, based on the logic of the Penman-Monteith equation, is calculated using daily meteorological reanalysis data and 8-day remotely sensed vegetation properties from MODIS as inputs (Mu et al., 2011). In arid and semi-arid regions, the Penman-Monteith equation has been found to overestimate ET by up to 20% because it assumes there is uniform vegetative coverage with a steady supply of water available to evaporate (Allen et al., 1998). In South Africa, MODIS ET has been shown to overestimate ET during dry seasons based on regional water balance and literature data (Jovanovic et al., 2015). However, the LRB lacks historical ET data thus this study used MODIS ET estimates to support monthly and annual water balance calculations from August 2009 to July 2019.

CHAPTER 3: METHODS

3.1 Catchment Water Balance and Infiltration Estimates

Hydrological inputs and outputs within a catchment are crucial to understanding groundwater storage changes and surface flow patterns. These interactions are generally observed via a simple water balance that considers the catchment a closed system. The primary water balance input is precipitation, but seasonally may include snowmelt or groundwater inflow contributions. Water balance outputs include stream/river flow, evapotranspiration, surface run-off, and groundwater movement. For the Sand River Basin, a water balance was generated to determine estimates of monthly changes in groundwater storage from August 2009 to July 2021 according to:

$$\Delta S = P - ET - R \qquad (1)$$

Where ΔS is change in storage, P is precipitation, ET is evapotranspiration, R is runoff, and all values are in m/month, adjusted by area of the catchment and time. Precipitation was the only input considered; monthly values from the results of the Thiessen polygon averaging method were used. ET and river flow were considered as outputs; MODIS ET data and river flow data from the gage at Waterpoort were used.

3.2 Groundwater Storage Estimates

Monthly groundwater storage changes were derived from GRACE TWS estimates using flow data, GLDAS soil moisture, and GLDAS plant canopy storage data products according to:

$$\Delta GWS = \Delta TWS - \Delta(SM + PC + R) \qquad (2)$$

where ΔGWS is change in groundwater storage, ΔTWS is change terrestrial water storage, SM is soil moisture, PC is plant canopy storage, and R is in runoff, all in meters. The resulting groundwater storage represents relative monthly storage.

3.4 Model Development

Hydrologic models have been increasingly used to estimate groundwater storage changes and observe the impact of climate variations on groundwater and monitor drought and wetness conditions (Botai et al., 2020; Crosbie et al., 2013; Li et al., 2019). Advanced models can provide spatially and temporally continuous groundwater storage estimates that reflect climate variations and are suitable for drought monitoring and prediction (Li et al., 2019). However, direct groundwater storage change estimates from models require high quality precipitation, simulated runoff, and reasonably accurate evapotranspiration estimates (Jiménez et al., 2011; Li et al., 2019; Mueller et al., 2011). Without access to historical records of in-situ data, modelled groundwater estimates may be oversimplified and inconsistent between various models or reality (Li et al., 2019; Xia et al., 2017).

Sustainable management of groundwater resources has traditionally been developed by examining field observations or constructing comprehensive numerical models (Ahmed, 2020; Ahmed et al., 2016). The construction of models is effective but requires a collection of broad field data (groundwater levels, hydraulic variables, lithologic data) that are challenging to find on a regular and high-quality. Field observations may not adequately represent the entire hydrogeologic area of interest. For instance, floodplain inundation, direct groundwater flow, and drainage into wetlands are some of the many basin outflow pathways that are not registered by conventional stream flow gauges. Hydrologic modelling is one method for resolving limitations of field data, providing future estimates of extreme climate events, and improving understanding

of hydrologic processes in a region. In this study, the Hydrologic Engineering Center's Hydrologic Modeling System (HEC-HMS) was used to simulate flow of the Sand River through the Soutpansberg Mountains watershed. HEC-HMS is a software developed by the U.S Army Corps of Engineers to simulate complete hydrologic processes of watershed systems (Feldman, 2000). The software includes traditional hydrologic analyses, such as infiltration, baseflow, unit hydrograph, and hydrologic routing. It also allows the user to input specified time series data. HEC-HMS was selected as the software for model development due to its parsimonious nature, amount of data input required, time scale, automated calibration capability, selection of methods for parameter calculation, and accuracy of results.

3.4.1 Watershed Delineation

Topography is an essential input for hydrological modeling. Terrain information defines watershed boundaries and shapes river networks to support parameters that are sensitive to hill slopes, such as surface flow travel times, runoff characteristics, and infiltration (Zhang et al., 2020). The SRTM DEMs (section 2.2.3) were processed using GIS software (QGIS 3.24) to extract terrain information and delineate the Sand River catchment within the Soutpansberg Mountains. The outlet for the watershed was selected as the location of the Waterpoort river gage. The delineated watershed covers 7,794 km^2 approximately 46% of the total area of the Sand River catchment (Figure 2). GIS processing steps for delineating the watershed include merging the DEMS, creating a depressionless DEM, extracting flow direction and accumulation, creating the watershed outlet point, identifying streams, and delineating the watershed boundaries. The depressionless DEM was inputted as terrain in HEC-HMS to geographically link model components.

3.4.2 HEC-HMS Workflow

The developed HEC-HMS model simulated flow at Waterpoort from August 2019 to July 2020; this period was selected based on in-situ data availability. Model development workflow is outlined in Figure 7. This study used the following embedded HEC-HMS analysis methods: baseflow recession method for baseflow analysis, a simple canopy interception model, the Soil Conservation Service Curve Number (SCS-CN) method for infiltration estimates, and the SCS unit hydrograph method for transform.

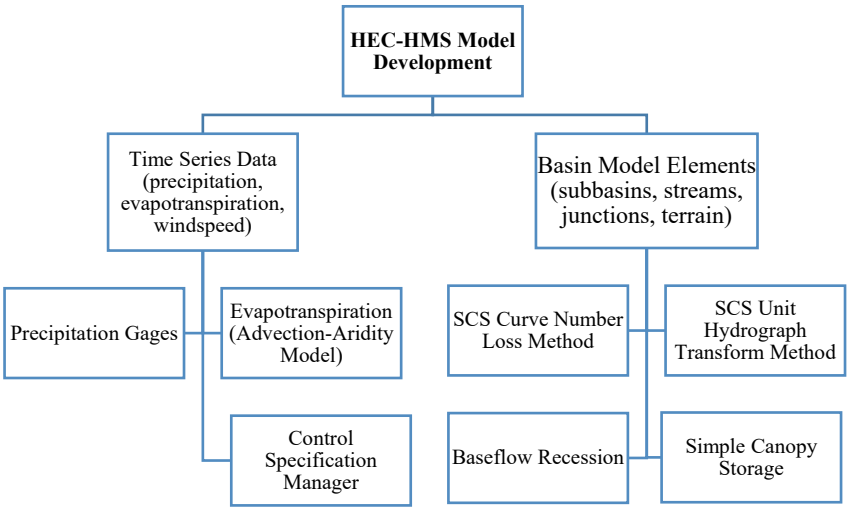

Figure 7. HEC-HMS model development workflow; HEC-HMS can be highly parameterized with the inclusion of both user-specified and software-generated data and methods.

HEC-HMS utilizes four basic components to generate a complete hydrologic model: the basin model, meteorological model, control specification model, and input time series. The components are linked by physical features of the watershed, such as terrain, streams, subbasins, outlet points, and junctions. Once basin elements are added or delineated, basin characteristics including slope, length of stream, and area of basin are shown by the model.

3.4.2 Model Domain

The domain for the developed model was generated in two scales (Figure 8). The first represents the entire delineated catchment of the Sand River at the Soutpansberg Mountains, with the outlet point at the location of the Waterpoort gage (Figure 8A). The second iteration of the model was simplified to subbasin one (Figure 8B), which was selected due to discussions with stakeholders and the availability of in-situ data from the Medike Nature Reserve hydrometeorological station within the subbasin area.

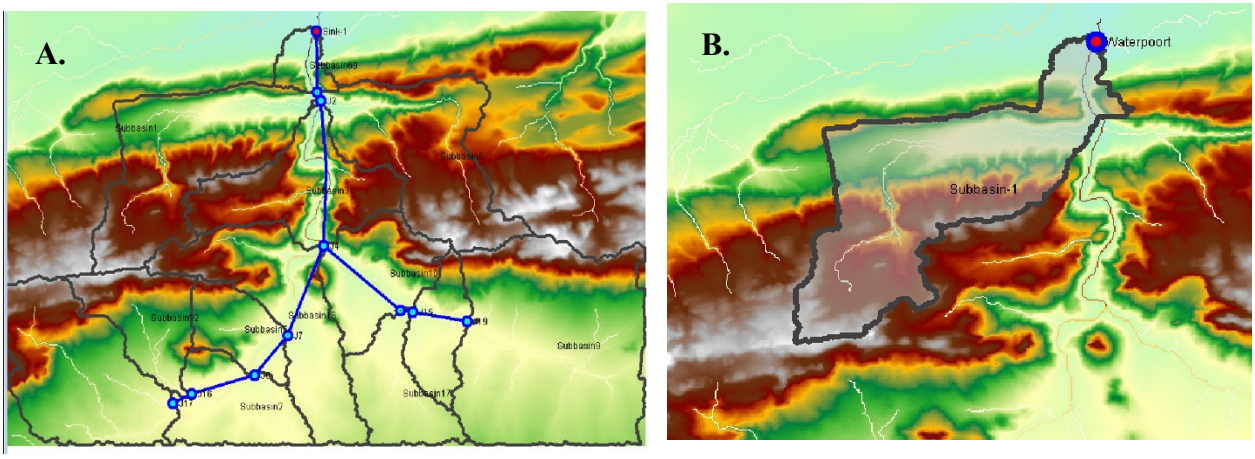

Figure 8. Terrain and model elements in HEC-HMS in two scales.

3.4.1 Baseflow

Baseflow is the portion of streamflow that exists in a stream without contribution of direct runoff from rainfall. Estimation of baseflow is useful in understanding the interaction of surface and sub-surface water. The baseflow recession model separates the baseflow from the hydrograph of total streamflow using a recession model based on the following:

$$Q(t) = Q_o e^{(\frac{-t-t_o}{k})} \quad (3)$$

where Q_o is the flow at initial time t and k is an exponential decay constant in the dimension of time (Chow et al., 1988). The baseflow recession method in HEC-HMS requires an initial discharge representing the baseflow (m^3/s), the recession constant, and a threshold type as either the ratio to peak or the threshold discharge (Feldman, 2000). This study used the ratio to peak method as threshold type. Baseflow parameter inputs were determined based on the flow data from the river gage at Waterpoort. As the Sand River does not have observed perennial flow, the baseflow and ratio to peak were set to zero.

3.4.2 Simply Canopy Interception Model

Canopy models represent plant cover across the model domain. Plants intercept precipitation, which reduces the amount that reaches the ground. The simple canopy method was selected for this model. All precipitation is intercepted until the canopy storage capacity is filled. Once the storage is filled, the remaining precipitation is assumed fall directly to the soil and infiltrate. All potential evapotranspiration empties the canopy storage until none is remaining. The inputs for this model are initial storage, representing the percentage of the canopy storage that is full of water at the beginning of the simulation, the maximum canopy storage, and the crop coefficient. For this study, the initial storage was 0%, the maximum storage was 8 mm, and the crop coefficient was 1.

3.4.3 Infiltration

Loss models are used to estimate the volume of runoff given precipitation and properties of the watershed. These are generally surface models and losses can occur by infiltration (Dvory et al., 2018). The SCS-CN method is used to estimate rainfall-runoff volume from precipitation

in small watersheds (Natural Resources Conservation Service, 1999; Soomro et al., 2019). The CN depends on soil type and land use and land cover of an area. CN is a parameter which estimated precipitation excess as a function of cumulative precipitation, soil cover, land use, and antecedent moisture according to:

$$P_e = \frac{(P - I_a)^2}{(P - I_a) + S} \quad (4)$$

where P_e is accumulated precipitation excess at time t, P is accumulated rainfall depth at time t, I_a is the initial loss (initial infiltration), and S is the potential maximum retention (ability of a watershed to retain storm precipitation). Until the accumulated rainfall exceeds the initial infiltration, P_e (runoff) is zero.

The CN for this study was determined to be 20 based on land cover data and associated curve numbers defined under arid and semi-arid rangelands with hydrologic soil group A and good coverage (USDA TR55). This CN was used to calculated HEC-HMS inputs for the SCS-CN method according to:

$$S = 25.4(\frac{1000}{CN} - 10) \quad (5)$$

$$I_a = 0.2 * S \quad (6)$$

where I_a is the initial loss (infiltration) and S is the potential maximum retention. Equation 6 is a dimensional equation to remain consistent with SI units.

3.4.4 Transform

The SCS hydrograph transform method was used to reproduce the direct runoff through additional rainfall over the watershed (Feldman, 2000). This hydrograph is a dimensionless, single-peaked model. The method related the hydrograph peak to time of hydrograph peak by:

$$U_p = C\frac{A}{T_p} \quad (7)$$

Where C is a conversion constant (2.08 for SI units), A is watershed area, and T_p is time of peak. T_p is related to the duration of the unit of excess precipitation by:

$$T_p = \frac{\Delta t}{2} + t_{lag} \quad (8)$$

Where Δt is the excess precipitation duration and t_{lag} is the basin lag. Basin lag is the time difference between the center of mass of excess rainfall to the hydrograph peak (Feldman, 2000). The lag time was estimated to be 50 minutes. In HEC-HMS, lag time is the only required input for this method. The SCS unit hydrograph method was selected because of its minimal input requirement and successful application in modeling watershed with variable land use and land cover (Soomro et al., 2019).

CHAPTER 4: RESULTS AND DISCUSSION

4.1 Borehole Drilling Depth

Aquifer characteristic information, elevation, borehole depth, and date of completion were analyzed for 438 boreholes from the SADC-GMI database in the Sand River Catchment.

Regional aquifer types are determined based on groundwater flow characteristics from lithological classes. The underlying lithography of the Sand River catchment based on the SADC-GMI borehole classification information is largely granite, syenite, gabbro, gneiss, and migmatites, with 76% of the boreholes in the catchment falling in this category (SADC-GMI, 2010a). The aquifer type for these boreholes is low permeability formations, where water can infiltrate but is limited by aquifer structure in low permeability areas. Drilling depth over time was calculated and examined by subtracting borehole depth from elevation (Figure 9). An increase in drilling depth over time corresponds to an increase in depth to the water table and would suggest that regional aquifer levels had decreased. However, due to the lack of data entries between 2003 and 2010, no conclusions about the depth to the water table during this period could be made from this dataset. Borehole entries were concentrated between the years 2000 and 2003. Only 16 boreholes were entered into the SADC-GMI database from 2003 to 2010. The lack of recent data and the static nature of the dataset reveal the significant limitations of using this dataset to inform groundwater resources management in the Sand River catchment.

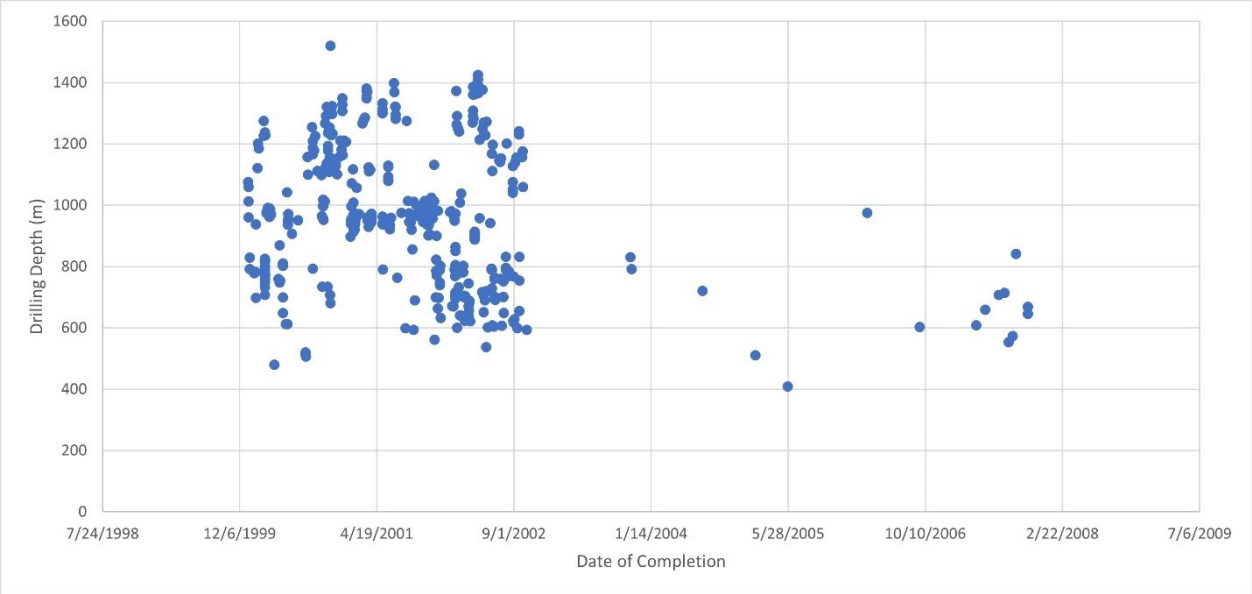

Figure 9. Drilling depth of 438 SADC-GMI boreholes in the Sand River Catchment from 2000-2010.

4.2 Catchment Water Balance and Groundwater Storage Estimates

4.2.1 Monthly Estimates

Monthly precipitation from DWS gages (Department of Water and Sanitation, 2011), evapotranspiration from MODIS (Running et al., 2022), and runoff from the DWS gage at Waterpoort (Department of Water and Sanitation, 2011) in the Sand River catchment were analyzed from August 2009 to August 2021 (Figure 10). Assessment of the individual elements shows a slight decrease in monthly precipitation and a significant decrease in runoff since hydrologic year 2015. These elements were used in a catchment water balance to estimate monthly changes in groundwater storage (Figure 11). Groundwater storage from the catchment water balance, relative monthly changes in groundwater storage derived from GRACE and GLDAS, and total change in terrestrial water storage from GRACE were compared (Figure 11). Groundwater storage estimates derived from GRACE and GLDAS have strong correlation with estimates from the catchment water balance ($r = 0.82$) (Figure 12). These results show that regional changes in groundwater storage largely respond to availability of rainfall, indicating that groundwater recharge likely takes place during or shortly after periods of heavy rainfall and follows the variability of precipitation interannually. During hydrologic years with less rainfall, monthly change in groundwater significantly decreases, with negative peaks in January 2013 and January 2015. These results indicate that the groundwater resources in the region are resilient to periods of drought due to the quick recharge capability of the aquifer.

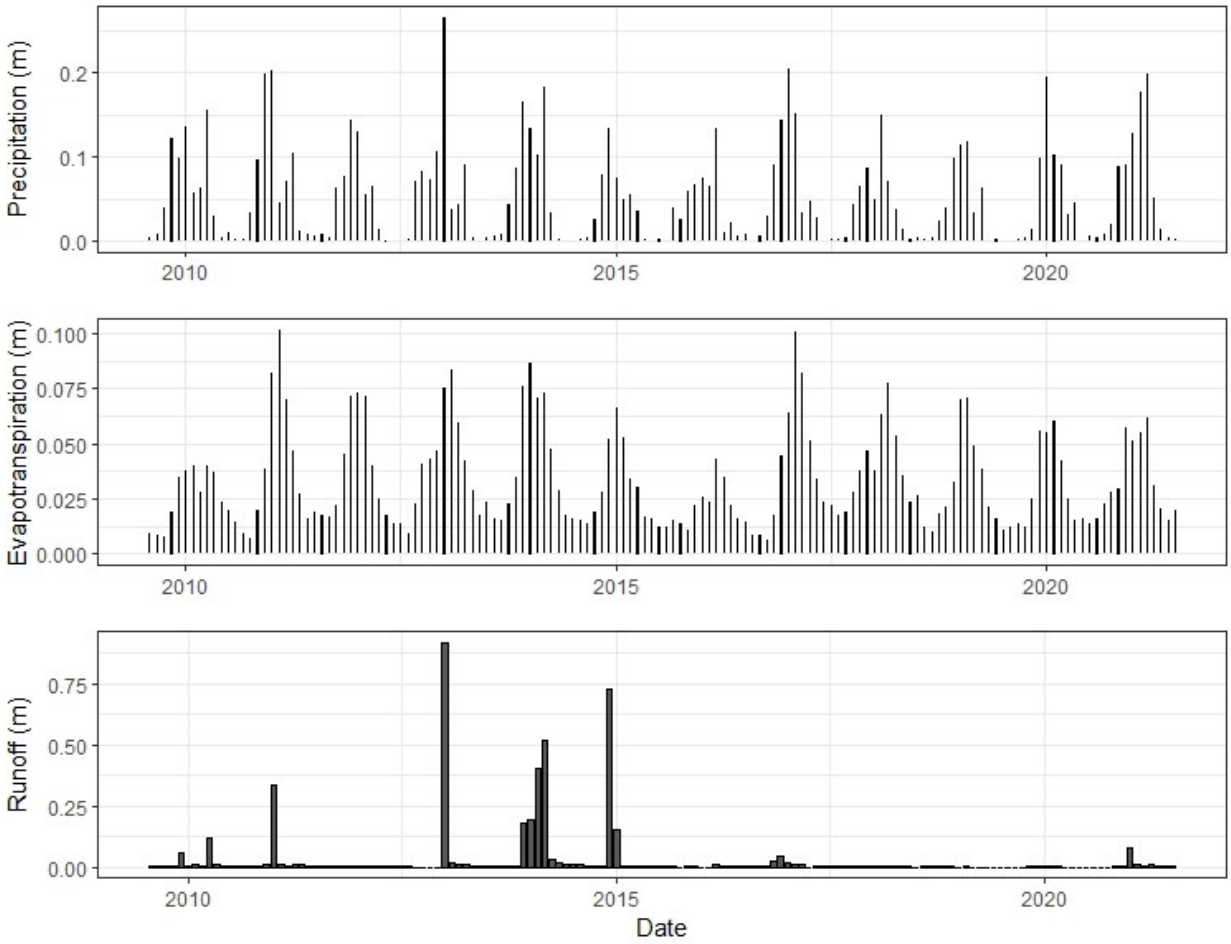

Figure 10. Individual components of the catchment water balance in meters shown monthly, from August 2009 - July 2021

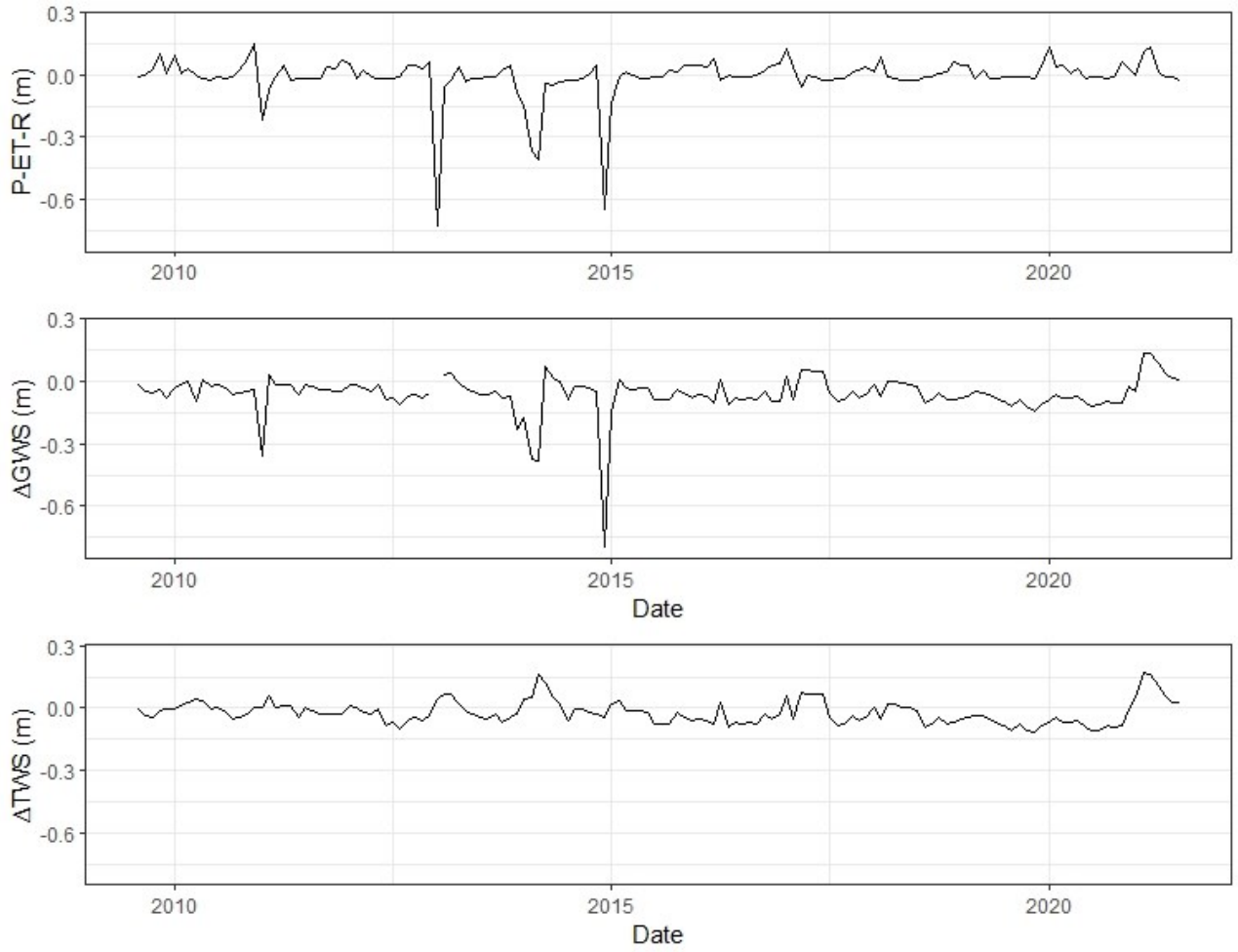

Figure 11. Estimates for monthly change in groundwater storage in meters. P-ET-R is the result of the catchment water balance, ΔGWS is the change in groundwater storage derived from GRACE, GLDAS, and runoff components, and ΔTWS is the monthly change in terrestrial water storage from GRACE.

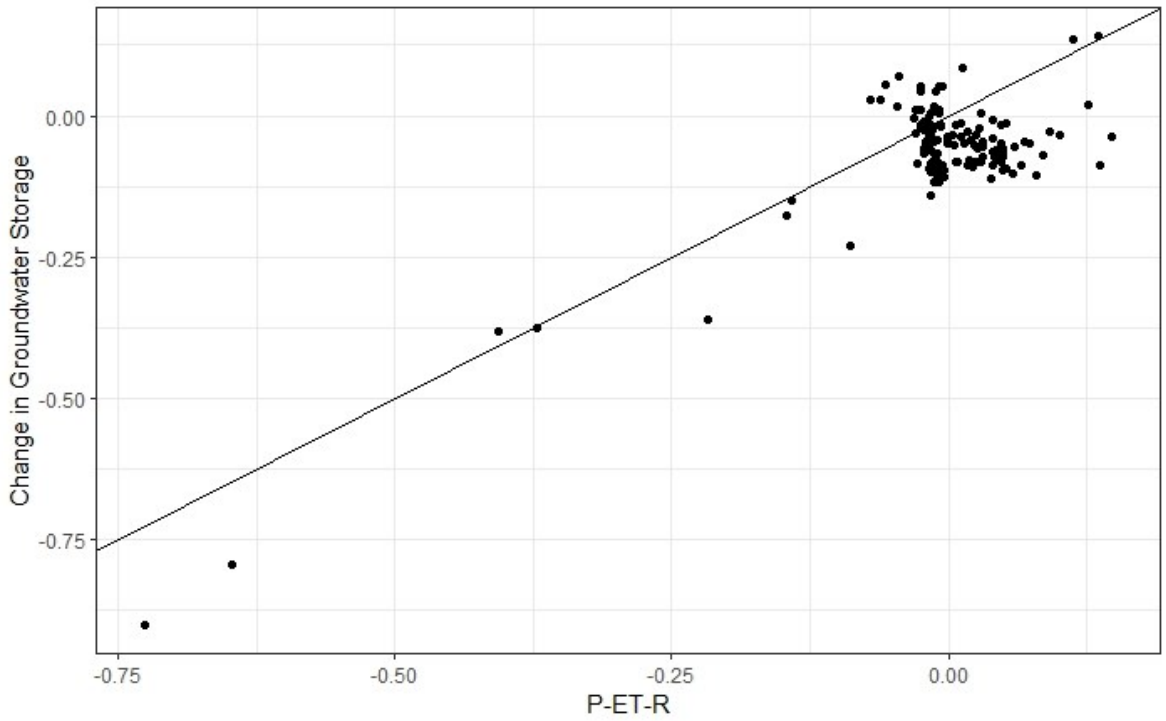

Figure 12. Comparison of remotely sensed and catchment water balance groundwater storage estimates.

4.2.2 MODIS Evapotranspiration vs. Calculated Evapotranspiration

MODIS evapotranspiration (8-day) and daily evapotranspiration calculated from the Advection-Aridity model were compared from August 2019 to July 2021 (Figure 13). The maximum daily average was 3.28 mm/day and 3.18 mm/day, and the minimum was 0.23 mm/day and 0 mm/day, obtained by MODIS and the advection-aridity model, respectively. MODIS outputs a higher minimum evapotranspiration value because the method used to derive evapotranspiration assumes there is always water available to evaporate. Monthly averages of the two datasets are not well correlated ($r = 0.42$) (Figure 14). Despite these limitations, MODIS evapotranspiration was selected for the water balance calculations in this study due to limited availability of data for the advection-aridity model calculations.

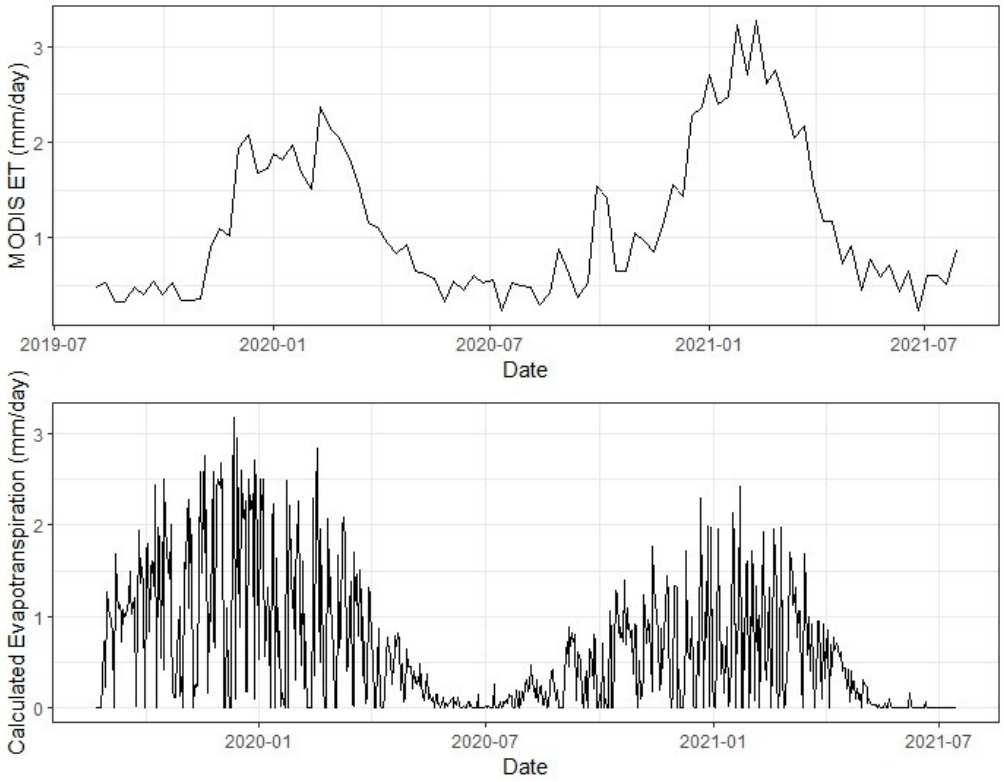

Figure 13. MODIS evapotranspiration and evapotranspiration calculated from the Advection-Aridity model.

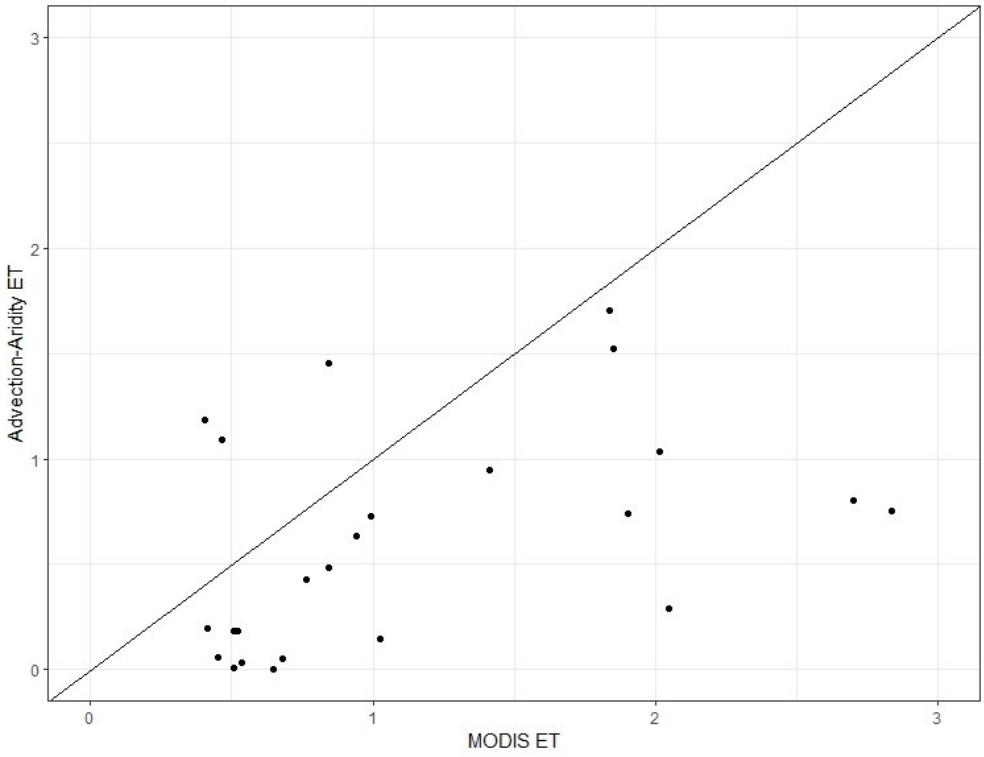

Figure 14. Comparison of MODIS and advection-aridity average monthly evapotranspiration values.

4.2.3 Annual Estimates

An annual catchment water balance was calculated for hydrologic years 2010 to 2021. The individual components were average annual precipitation, annual evapotranspiration from MODIS, and annual runoff from the gage at Waterpoort (Figure 15). The annual results of the catchment water balance show a significant decrease in change in groundwater storage and annual runoff after hydrologic year 2015. Both of these decreases could be a result of reliance on groundwater during the period of low precipitation from hydrologic years 2014 and 2015. Additionally, evaporation rates since 2015 (relative to the amount of precipitation) may be higher than in previous years due to global temperature rise, which also has an impact on available surface water resources.

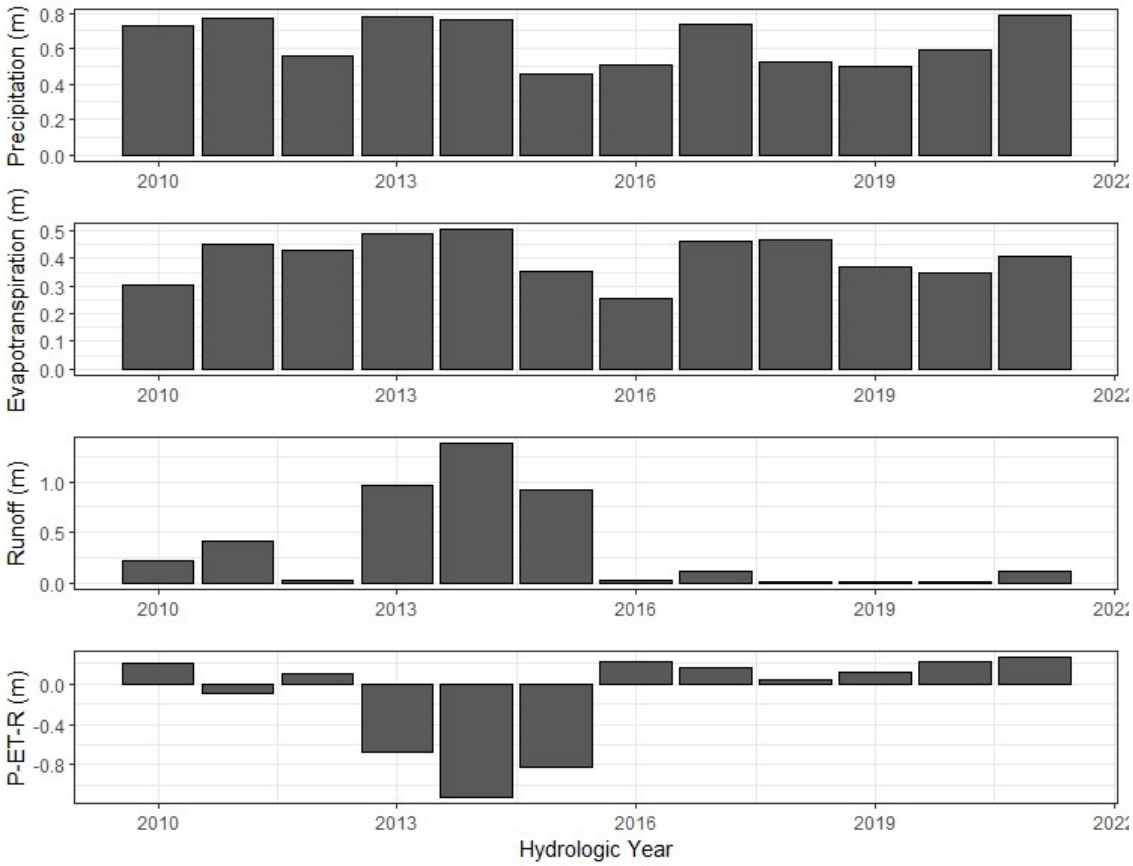

Figure 15. Annual values for each component and results of the catchment water balance.

4.3 HEC-HMS Model Results

4.3.1 Modelled Flow

The HEC-HMS total flow output was compared to the observed flow from the gage at Waterpoort (Figure 16). Qualitatively, the modelled and actual flow are similar. In most cases, the actual flow is higher than the model likely due to flow from the rest of the watershed. Discrepancies may also be due to the complexity of modeling baseflow, missing contributions of groundwater, or interception of the precipitation not being captured by the simple canopy mode.

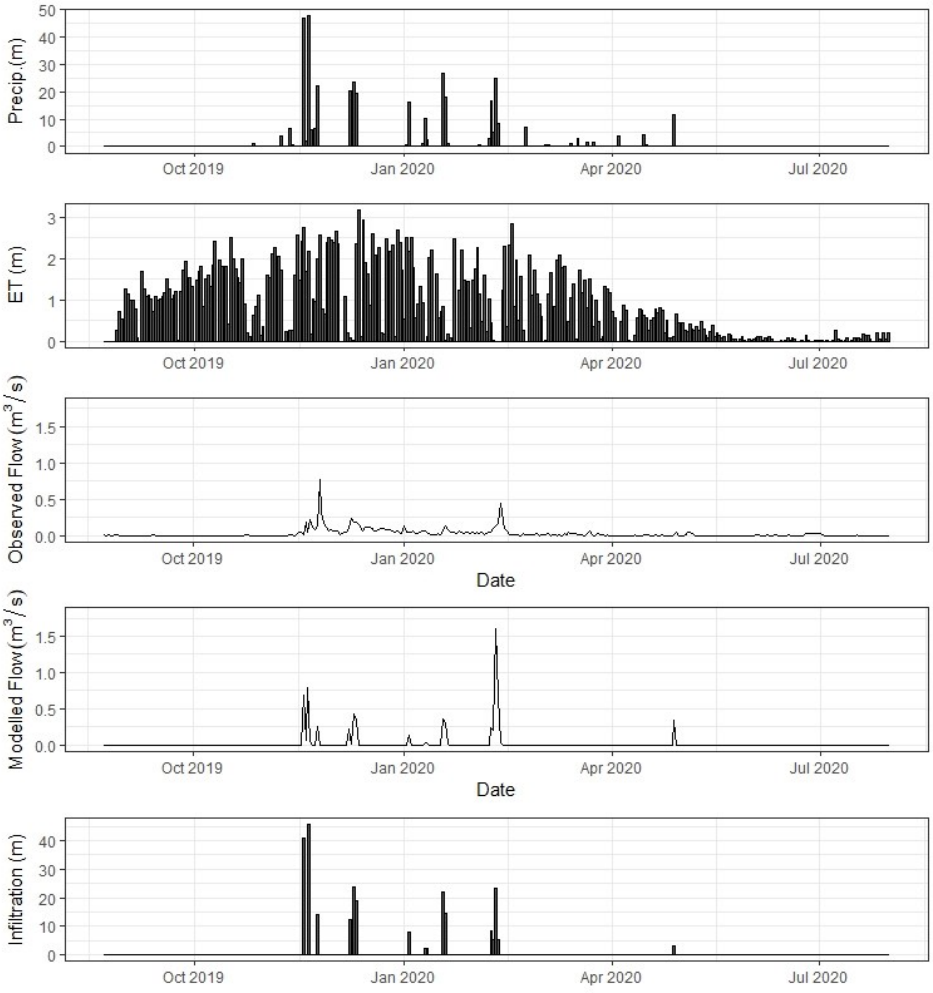

Figure 16. HEC-HMS modelled flow, observed flow from the gage at Waterpoort, and meteorological inputs, shown daily for the hydrologic year 2019 to 2020. Precipitation is from the Medike weather station and evapotranspiration from the advection aridity model.

4.3.2 Modelled Infiltration and Changes in Groundwater Storage

Monthly modelled infiltration values were compared to the results from the catchment water balance and ΔGWS values, derived from GRACE terrestrial water storage, GLDAS soil moisture and plant canopy storage, and runoff from the gage at Waterpoort, from August 2019 to July 2020 (Figure 17). The maximum infiltration during this time period was 8.07 million cubic meters in November 2019. Figure 19 also shows that as infiltration increases in the subbasin from October to March, there is a steady increase in monthly groundwater storage changes from November to April. The total infiltration in the subbasin was 20.2 million cubic meters from August 2019 to July 2020. This total represents approximately 10% of the water demand for the Sand River catchment. Additionally, since the area of the Soutpansberg Mountains in the Sand River catchment is more than twice the size of subbasin 1, the contribution of groundwater from the Soutpansberg Mountains is likely much greater.

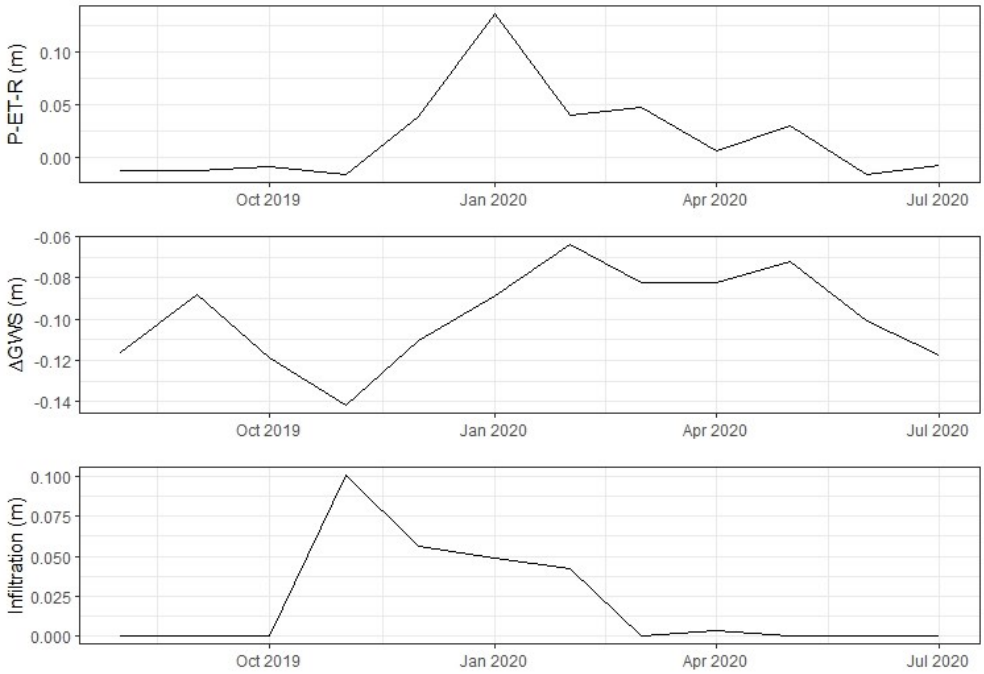

Figure 17. Comparison of monthly modelled infiltration, ΔGWS from GRACE and GLDAS components, and the groundwater storage results from the water balance calculations.

4.3.3 Model Sensitivity Analysis

During model development, it is important to analyze model response to input parameter changes as part of the verification and evaluation of model results. Sensitivity analyses are the first step in this process because the results suggest where the data collection efforts should focus, what degree of care should be taken for parameter estimates, and the relative importance of the various parameters utilized. Land cover, land use, and soil type data used to support CN calculations may vary greatly over an area of land. Thus, a range of values for CN were used to analyze the sensitivity of the developed model. The CN sensitivity analysis was conducted to observe the impact of varying CN on excess runoff from precipitation events. The model was run for CN values of 10, 35, 50, 75, and 90, keeping all other parameters unchanged. Modelled infiltration and modelled flow are shown (Figure 18, Figure 19). When using inputs derived from CN 90, the maximum discharge was 30.55 m^3/s and the maximum monthly infiltration was 25.71 mm in November 2019. At CN 10, the maximum discharge was 0.69 m^3/s and the maximum infiltration was 90.24 mm in November 2019. The range in resulting runoff values indicates a high sensitivity of the model to CN.

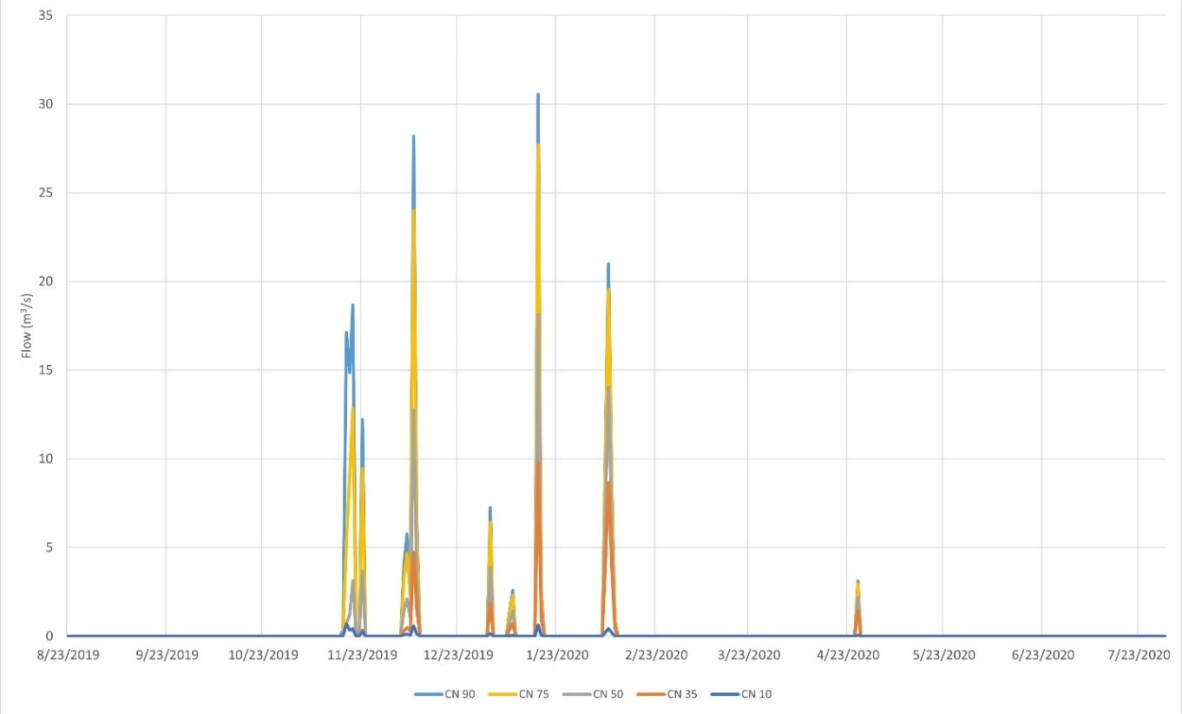

Figure 18. Sensitivity of daily, modelled flow to varying CN.

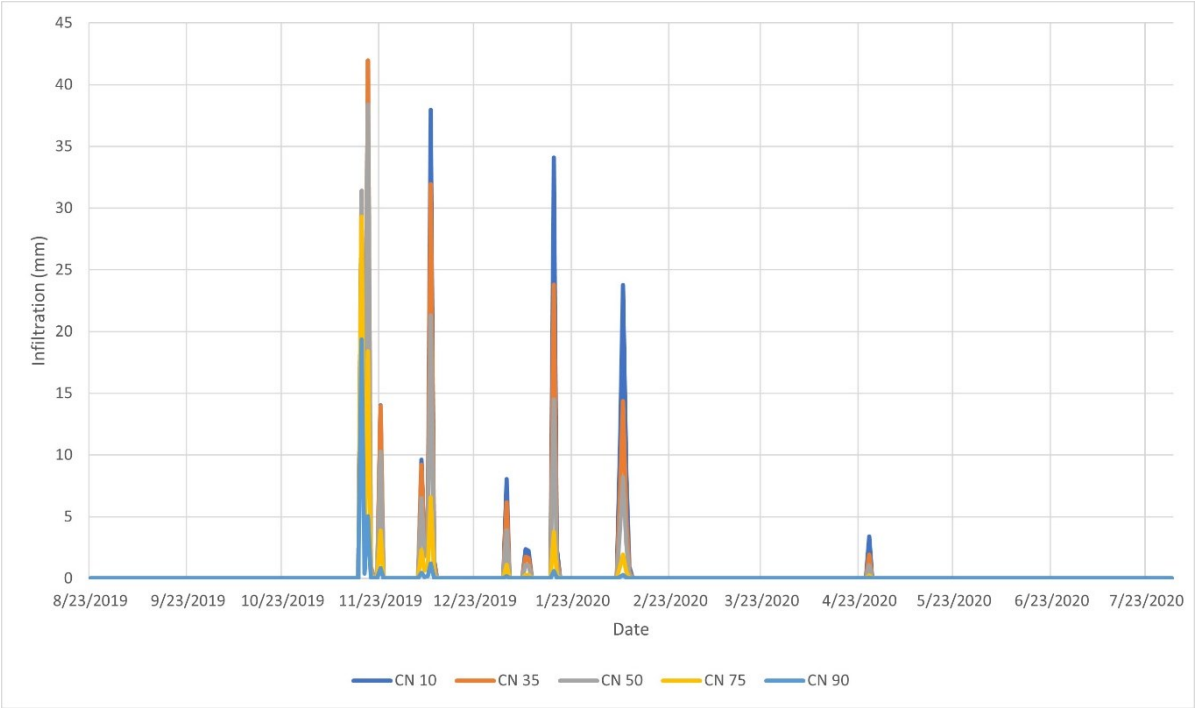

Figure 19. Sensitivity of daily, modelled infiltration to varying CN.

CHAPTER 5: CONCLUSION

The objectives of this study were to determine the potential for using hydrologic modelling and remotely sensed data to evaluate groundwater resources in a data-scarce region and to show that the Soutpansberg Mountains act as high elevation water towers for the downstream area of the Sand River catchment. The combined approach of hydrologic modelling and remotely sensed data to assess groundwater resources proved successful; the study results show that despite variations in precipitation interannually and increased used of groundwater during periods of less precipitation, monthly changes in groundwater storage have remained relatively stable over time. There is no significant increasing or decreasing trend in changes in groundwater storage. This indicates groundwater resilience. Additionally, when monthly changes in groundwater storage were compared to modelled infiltration, the results confirm that when there are peaks in precipitation and infiltration, the monthly change in groundwater storage also increases. The modelled infiltration results also suggest there is more groundwater present in the Soutpansberg Mountains than what has previously been unaccounted for; the consensus has been that there are insufficient groundwater resources to support regional development.

The results of this study show that there are significant groundwater resources available which require monitoring and management. The use of a water balance and hydrological modelling approach supplemented with remote sensing data can aid in estimating groundwater resources in unmonitored catchments; however, there are several limitations in this study that present challenges when interpreting the results and providing guidance for regional water resources management. The largest limitation is the lack of current and historical in-situ groundwater monitoring data in both the Sand River catchment and LRB for model validation. However, studies have shown that the individual use of any of these methods may be effective in

filling regional knowledge gaps globally, especially in LMIC and transboundary river basins. By combining these approaches for groundwater resources estimates and using as much in-situ data as possible (precipitation, runoff, and calculated ET), confidence in the results of this study is increased.

The groundwater storage estimates derived from GRACE and GLDAS data products have a high spatial resolution. The spatial resolution of GRACE (0.5˚ by 0.5˚ grid) is much higher than the area of the Sand River watershed in the Soutpansberg Mountains. These results may not effectively demonstrate groundwater and surface water interactions unique to this region. The water balance calculations for this study are simple and do not consider interception of precipitation from vegetation, groundwater extraction, streamflow diversion, or a baseflow contribution. The simplicity of these calculations is effective for observing trends and initial observations of infiltration, but the infiltration results cannot be used as a standard for the water that is available to support regional water demand. Analysis of ERT results (see appendix) supports the presence of groundwater, which supplies Sand River tributaries in the Soutpansberg Mountains; however further investigation is warranted. Improved understanding of these resources can support the conservation of these groundwater resources and downstream development. Specifically, with pressure to increase development around Musina (located downstream at the confluence of the Sand and Limpopo Rivers), improved understanding of available water resources can help decision makers create a sustainable water budget for the region.

HEC-HMS was selected for its parsimonious nature, amount of data input required, time scale, automated calibration capability, selection of methods for parameter calculation, and accuracy of results. However, as with all simulation systems, there are limitations. The main

limitations of using HEC-HMS stems from aspects of its design: simplified flow formulation and simplified flow representation. The model uses constant parameter values, which may change over time in a watershed. The simplified nature of these computations allows for quick simulations and precise results but may contribute to the disparities observed between the modelled flow and observed flow at Waterpoort in the model developed for the Soutpansberg Mountains watershed. Additionally, the results of the HEC-HMS model vary from the groundwater storage estimates derived from GRACE and the catchment water balance because the model only considers a subset of the catchment.

5.1 Management Implications and Future Work

The results of this study find that the Soutpansberg Mountains act as high elevation water towers and show there is a complex-unmonitored subsurface flow occurring at the Sand River catchment within mountains. It was determined that the infiltration estimates are likely contributing to sub-surface flow as opposed to deep groundwater recharge due to the low permeability characterization of regional aquifers. The exact contribution of these water resources to the baseflow of the Sand River was not determined, but would be useful for a range of water resources management applications including:

- Maintaining regional water security
- Increasing sustainability of water supply
- Improving accuracy of water resource assessments
- Improving understanding of groundwater recharge, and
- Determining rainfall thresholds that cause surface flows and recharge.

Therefore it is recommended that additional work is done to characterize the subsurface flow, determine the contribution to the baseflow of the Sand River, and begin monitoring groundwater

resources in the Soutpansberg Mountains. Groundwater data collection is the top priority, as none of these results can be fully validated without this data. It would also be useful to determine an estimate for monthly groundwater abstraction to help define sustainable groundwater use in the region. Remote sensing may be useful for the examination of vegetation, and thus, transpiration, activity in the area that does not match precipitation. This could be done with the normalized difference vegetation index (NDVI) from many multispectral satellites (red and near-infrared bands are needed) and precipitation from ground-based measurement or the global precipitation (GPM) mission (Hou et al., 2014). Additionally, river flow estimates have been made with 3-meter Planet Labs data (Martin et al., 2018) or Sentinel (Walker et al., 2019).

REFERENCES

Abiye, T. A., & Leketa, K. C. (2021). The need for managing historic groundwater in the Limpopo River Basin, southern Africa: based on the δ18O, δ2H and 14C data. *Groundwater for Sustainable Development*, *14*. https://doi.org/10.1016/j.gsd.2021.100583

Ahmed, M. (2020). Sustainable management scenarios for northern Africa's fossil aquifer systems. *Journal of Hydrology*, *589*. https://doi.org/10.1016/j.jhydrol.2020.125196

Ahmed, M., Sultan, M., Yan, E., & Wahr, J. (2016). Assessing and Improving Land Surface Model Outputs Over Africa Using GRACE, Field, and Remote Sensing Data. In *Surveys in Geophysics* (Vol. 37, Issue 3, pp. 529–556). Springer Netherlands. https://doi.org/10.1007/s10712-016-9360-8

Alemaw, B. F. (2012). Hydrological Modeling of Large Drainage Basins Using a GIS-based Hybrid Atmospheric and Terrestrial Water Balance (HATWAB) Model. *Journal of Water Resource and Protection*, *04*(07), 516–522. https://doi.org/10.4236/jwarp.2012.47060

Allen, R. G., Pereira, L. S., Raes, D., & Smith, M. (1998). Crop Evapotranspiration - Guidelines for computing crop water requirements. *FAO Irrigation and Drainage Paper*. https://www.fao.org/3/x0490e/x0490e00.htm#Contents

Beaudoing, H., & Rodell, M. (2020). *GLDAS Noah Land Surface Model L4 monthly 0.25 x 0.25 degree V2.1*. Goddard Earth Science Data and Information Services Center (GES DISC). https://doi.org/10.5067/SXAVCZFAQLNO

Beaudoing, H., & Rui, H. (2021). *README Document for NASA GLDAS Version 2 Data Products*.

Bhanja, S. N., & Mukherjee, A. (2019). In situ and satellite-based estimates of usable groundwater storage across India: Implications for drinking water supply and food security. *Advances in Water Resources*, *126*, 15–23. https://doi.org/10.1016/j.advwatres.2019.02.001

Blanchy, G., Saneiyan, S., Boyd, J., McLachlan, P., & Binley, A. (2020). ResIPy, an intuitive open source software for complex geoelectrical inversion/modeling. *Computers and Geosciences*, *137*. https://doi.org/10.1016/j.cageo.2020.104423

Botai, C. M., Botai, J. O., Zwane, N. N., Hayombe, P., Wamiti, E. K., Makgoale, T., Murambadoro, M. D., Adeola, A. M., Ncongwane, K. P., de Wit, J. P., Mengistu, M. G., & Tazvinga, H. (2020). Hydroclimatic extremes in the limpopo river basin, south africa, under changing climate. *Water (Switzerland)*, *12*(12). https://doi.org/10.3390/w12123299

Bouchet, R. J. (1963). Actual evapotranspiration, potential evapotranspiration, and agricultural production. *Annales Agronomiques*, *14*(5), 743–824.

Brutsaert, W., & Stricker, H. $. (1979). *An Advection-Aridity Approach to Estimate Actual Regional Evapotranspiration* (Vol. 15, Issue 2).

Chanu, C. S., Munagapati, H., Tiwari, V. M., Kumar, A., & Elango, L. (2020). Use of GRACE time-series data for estimating groundwater storage at small scale. In *Journal of Earth System Science* (Vol. 129, Issue 1). Springer. https://doi.org/10.1007/s12040-020-01465-2

Chinoda, G., Moyce, W., Matura, N., & Owen, R. (2009). *Integrated Water Resource Management for Improved Rural Livelihoods: Managing risk, mitigating drought, and improving water productivity in the water scarce Limpopo River Basin*.

Chow, V. te, Maidment, D. R., & Mays, L. W. (1988). *Applied hydrology*. McGraw-Hill.

Cooley, S. S., Landerer, F. W., Humphrey, V., Reager, J. T., & Srinivasan, M. M. (2020). *GRACE L-3 Product User Handbook GRACE D-103133*.

CPWF. (2014). *Summary of the Challenge Program on Water and Food Research (CPWF) in the Limpopo River Basin*. www.seimapping.org/tagmi

Crosbie, R. S., Scanlon, B. R., Mpelasoka, F. S., Reedy, R. C., Gates, J. B., & Zhang, L. (2013). Potential climate change effects on groundwater recharge in the High Plains Aquifer, USA. *Water Resources Research*, *49*(7), 3936–3951. https://doi.org/10.1002/wrcr.20292

Department of Forestry Fisheries and the Environment. (2018). *South Africa National Land-Cover Datasets*. https://egis.environment.gov.za/sa_national_land_cover_datasets

Department of Water and Sanitation. (2011). *Hydrological Information System* . https://www.dws.gov.za/Hydrology/default.aspx

Dvory, N. Z., Ronen, A., Livshitz, Y., Adar, E., Kuznetsov, M., & Yakirevich, A. (2018). Quantification of groundwater recharge from an ephemeral stream into a mountainous karst aquifer. *Water (Switzerland)*, *10*(1). https://doi.org/10.3390/w10010079

Earle, A., Malzbender, D., Turton, A., & Manzungu, E. (2005). *A Preliminary Basin Profile of the Orange/Senqu River*.

Earle, Anton. (2006). *Indigenous and institutional profile : Limpopo River Basin*. International Water Management Institute.

Environmentek-CSIR. (2003). *Protection and Strategic Uses of Groundwater Resources in Drought Prone Areas of the SADC Region*.

Fathy, I., Abd-Elhamid, H., Zelenakova, M., & Kaposztasova, D. (2019). Effect of topographic data accuracy on watershed management. *International Journal of Environmental Research and Public Health*, *16*(21). https://doi.org/10.3390/ijerph16214245

Feldman, A. (2000). *Hydrologic Modeling System HEC-HMS Technical Reference Manual CPD-74B*.

Frappart, F., & Ramillien, G. (2018). Monitoring groundwater storage changes using the Gravity Recovery and Climate Experiment (GRACE) satellite mission: A review. In *Remote Sensing* (Vol. 10, Issue 6). MDPI AG. https://doi.org/10.3390/rs10060829

Global Environment Facility. (2019). *Integrated Transboundary River Basin Management for the Sustainable Development of the Limpopo River Basin*. https://gefportal.worldbank.org

Hou, A. Y., Kakar, R. K., Neeck, S., Azarbarzin, A. A., Kummerow, C. D., Kojima, M., Oki, R., Nakamura, K., & Iguchi, T. (2014). The Global Precipitation Measurement Mission. *Bulletin of the American Meteorological Society*, *95*(5), 701–722. https://doi.org/10.1175/BAMS-D-13-00164.1

IGRAC. (2020). *A global overview of quantitative groundwater monitoring networks*.

Jamaluddin, & Umar, E. P. (2018). Identification of subsurface layer with Wenner-Schlumberger arrays configuration geoelectrical method. *IOP Conference Series: Earth and Environmental Science*, *118*(1). https://doi.org/10.1088/1755-1315/118/1/012006

Jiang, D., Wang, J., Huang, Y., Zhou, K., Ding, X., & Fu, J. (2014). The review of GRACE data applications in terrestrial hydrology monitoring. In *Advances in Meteorology* (Vol. 2014). Hindawi Publishing Corporation. https://doi.org/10.1155/2014/725131

Jiménez, C., Prigent, C., Mueller, B., Seneviratne, S. I., McCabe, M. F., Wood, E. F., Rossow, W. B., Balsamo, G., Betts, A. K., Dirmeyer, P. A., Fisher, J. B., Jung, M., Kanamitsu, M., Reichle, R. H., Reichstein, M., Rodell, M., Sheffield, J., Tu, K., & Wang, K. (2011). Global intercomparison of 12 land surface heat flux estimates. *Journal of Geophysical Research Atmospheres*, *116*(2). https://doi.org/10.1029/2010JD014545

Jovanovic, N., Mu, Q., Bugan, R. D., & Zhao, M. (2015). Dynamics of MODIS Evapotranspiration in South Africa. *Water SA*, *41*(1), 79–90. https://doi.org/10.4314/wsa.v41i1.11

Kahler, D. M., Edokpayi, J. N., & Rose, K. C. (2019). *WATERQ2: UNDERSTANDING WATER QUALITY & QUANTITY IN THE LIMPOPO BASIN Hydrometeorological Station Network*.

Kahler, David. M. (2020). *Limpopo Resilience Lab: Medike Nature Preserve Dataset*. USAID Data Development Library. https://data.usaid.gov/d/chfb-yzu5.

Kollert, P. (1969). Groundwater Exploration by Electrical Resistivity Method. *Geophysical Memorandum*, *3*.

Landerer. (2021). TELLUS_GRAC_L3_CSR_RL06_LND_v04. . *PO.DAAC*.

Landerer, F. W., Flechtner, F. M., Save, H., Webb, F. H., Bandikova, T., Bertiger, W. I., Bettadpur, S. v., Byun, S. H., Dahle, C., Dobslaw, H., Fahnestock, E., Harvey, N., Kang, Z., Kruizinga, G. L. H., Loomis, B. D., McCullough, C., Murböck, M., Nagel, P., Paik, M., … Yuan, D. N. (2020). Extending the Global Mass Change Data Record: GRACE Follow-On Instrument and Science Data Performance. *Geophysical Research Letters*, *47*(12). https://doi.org/10.1029/2020GL088306

Landerer, & Swenson, S. C. (2012). Accuracy of scaled GRACE terrestrial water storage estimates. *Water Resources Research*, *48*. http://doi.org/10.1029/2011WR011453

Li, B., Rodell, M., Kumar, S., Beaudoing, H. K., Getirana, A., Zaitchik, B. F., de Goncalves, L. G., Cossetin, C., Bhanja, S., Mukherjee, A., Tian, S., Tangdamrongsub, N., Long, D., Nanteza, J., Lee, J., Policelli, F., Goni, I. B., Daira, D., Bila, M., … Bettadpur, S. (2019). Global GRACE Data Assimilation for Groundwater and Drought Monitoring: Advances and Challenges. *Water Resources Research*, *55*(9), 7564–7586. https://doi.org/10.1029/2018WR024618

Limpopo Basin Permanent Technical Committee. (2010). *Joint Limpopo River Basin Study Scoping Phase - Final Report*.

Love, D., Owen, R., Uhlenbrook, S., & van der Zaag, P. (2008). *The Mushawe meso-alluvial aquifer, Limpopo Basin, Zimbabwe: an example of the development potential of small sand rivers*.

Martin. (2021). *Department of Water and Sanitation GIS Data*. ArcGIS Online. https://gia.dws.gov.za/portal/home/item.html?id=487d74ecf16a434c9ec7867297ee4666

Martin, M. L., Glancey, K. M., & Kahler, D. M. (2018). Method Development for Remote Sensing of River Flow with Limited Ground-Based Measurements. . *AGU Fall Meeting*, H43G-2504.

Mocko, D. M. (2012). *NLDAS Noah Land Surface Model L4 Monthly 0.125 x 0.125 degree v2.1*. Goddard Earth Sciences Data and Information Services Center (GES DISC). https://doi.org/10.5067/WB224IA3PVOJ

Mosase, E. N. (2018). *Modeling Water Availability, Risk, and Resilience in a Semi-Arid Basin in Southern Africa*. https://openprairie.sdstate.edu/etdhttps://openprairie.sdstate.edu/etd/3180

Mu, Q., Heinsch, F. A., Zhao, M., & Running, S. W. (2011). Improvements to a MODIS global terrestrial evapotranspiration algorithm. *Remote Sensing of Environment*, *115*. https://doi.org/10.1016/j.rse.2007.04.015

Mueller, B., Seneviratne, S. I., Jimenez, C., Corti, T., Hirschi, M., Balsamo, G., Ciais, P., Dirmeyer, P., Fisher, J. B., Guo, Z., Jung, M., Maignan, F., McCabe, M. F., Reichle, R., Reichstein, M., Rodell, M., Sheffield, J., Teuling, A. J., Wang, K., … Zhang, Y. (2011).

Evaluation of global observations-based evapotranspiration datasets and IPCC AR4 simulations. *Geophysical Research Letters*, *38*(6). https://doi.org/10.1029/2010GL046230
NASA JPL. (2013). NASA Shuttle Radar Topography Mission Global 1 arc second Digital Elevation Model. *NASA EOSDIS Land Processes DAAC*. https://doi.org/10.5067/MEaSUREs/SRTM/SRTMGL1.003
NASA JPL. (2022). *Excluded days - GRACE*. https://grace.jpl.nasa.gov/data/grace-months/
Natural Resources Conservation Service. (1999). SCS Runoff Equation. *Unite States Department of Agriculture*.
Neves, M. C., Nunes, L. M., & Monteiro, J. P. (2020). Evaluation of GRACE data for water resource management in Iberia: a case study of groundwater storage monitoring in the Algarve region. *Journal of Hydrology: Regional Studies*, *32*. https://doi.org/10.1016/j.ejrh.2020.100734
Nicholson, S. E., Nash, D. J., Chase, B. M., Grab, S. W., Shanahan, T. M., Verschuren, D., Asrat, A., Lézine, A. M., & Umer, M. (2013). Temperature variability over Africa during the last 2000 years. *Holocene*, *23*(8), 1085–1094. https://doi.org/10.1177/0959683613483618
Penman, H. L. (1948). Natural evaporation from open water, bare soil, and grass. *Royal Society Publishing*. https://doi.org/10.0198/rspa.1948.0037
Pennsylvania State University (PSU). (2006). *1-km Multi-Layer Soil Characteristics Dataset. Version 1.0*. UCAR/NCAR Earth Observing Laboratory. https://data.eol.ucar.edu/dataset/8.43
Petrie, B., Chapman, A., Midgley, A., & Parker, R. (2014). *Climate Change, water and biodiversity-a synthesis*.
Priestley, C. H. B., & Taylor, R. J. (1972). On the assessment of surface heat flux and evaporation using large-scale parameters. *Monthly Weather Review*. https://doi.org/10.1175/1520-0493(1972)100%3C0081:OTAOSH%3E2.3.CO;2
Purdy, A. J., David, C. H., Sikder, M. S., Reager, J. T., Chandanpurkar, H. A., Jones, N. L., & Matin, M. A. (2019). An Open-Source Tool to Facilitate the Processing of GRACE Observations and GLDAS Outputs: An Evaluation in Bangladesh. *Frontiers in Environmental Science*, *7*. https://doi.org/10.3389/fenvs.2019.00155
Ramoeli, P., Katai, O., Lekgowe, O., Magowe, /, & Hydrogeologists, M. (2010). *Southern Africa Development Community (SADC) Hydrogeological Mapping Project*.
RESILIM. (2017). *Resilience in the Limpopo River Basin (RESILIM) Program*.
Rodell, Houser, P. R., Jambor, U., Gottschalck, J., Mitchell, K., Meng, C., Arsenault, K., Cosgrove, B., Radakovich, J., Bosilovich, M., Entin, J. K., Walker, J. P., Lohmann, D., & Toll, D. (2004). *The Global Land Data Assimilation System*. https://doi.org/10.1
Rodell, M., & Famiglietti, J. S. (2001). An analysis of terrestrial water storage variations in Illinois with implications for the Gravity Recovery and Climate Experiment (GRACE). *Water Resources Research*, *37*(5), 1327–1339. https://doi.org/10.1029/2000WR900306
Rodell, M., Velicogna, I., & Famiglietti, J. S. (2009). Satellite-based estimates of groundwater depletion in India. *Nature*, *460*(7258), 999–1002. https://doi.org/10.1038/nature08238
Rohde, M. M., Saito, L., & Smith, R. (2020). *Groundwater Thresholds for Ecosystems A Guide for Practitioners*. www.GroundwaterResourceHub.org.
Running, S., Mu, Q., & Zhao, M. (2022, June 17). *MODIS/Terra Net Evapotranspiration 8-Day L4 Global 500m SIN Grid V061*. NASA EOSDIS Land Processes DAAC. DOI: 10.5067/MODIS/MOD16A2.061

Rzepecka, Z., & Birylo, M. (2020a). Groundwater storage changes derived from GRACE and GLDAS on smaller river basins—a case study in Poland. *Geosciences (Switzerland)*, *10*(4). https://doi.org/10.3390/geosciences10040124

Rzepecka, Z., & Birylo, M. (2020b). Groundwater storage changes derived from GRACE and GLDAS on smaller river basins—a case study in Poland. *Geosciences (Switzerland)*, *10*(4). https://doi.org/10.3390/geosciences10040124

SADC. (2022). *Southern African Development Community (SADC)*. https://www.sadc.int/about-sadc/

SADC-GMI. (2010a). *Borehole Database (2010) - South Africa*. SADC Hydrogeological Mapping Project. https://sadc-gip.org/maps/391

SADC-GMI. (2010b). *SADC Groundwater Information Portal*. SADC Groundwater Management Institute. https://sadc-gip.org/

SADC-GMI. (2020). *2019-2020 Southern African Development Community-Groundwater Management Institute (SADC-GMI)*.

SADC-GMI. (2021, November). *Sustainable Groundwater Management Project, Phase 2*. SADC-GMI. https://sadc-gmi.org/projects/phase-2/

Saveca, P. S. L., Abi, A., Stigter, T. Y., Lukas, E., & Fourie, F. (2022). Assessing Groundwater Dynamics and Hydrological Processes in the Sand River Deposits of the Limpopo River, Mozambique. *Frontiers in Water*, *3*. https://doi.org/10.3389/frwa.2021.731642

Soomro, A. G., Babar, M. M., Memon, A. H., Zaidi, A. Z., Ashraf, A., & Lund, J. (2019). Sensitivity of Direct Runoff to Curve Number Using the SCS-CN Method. *Civil Engineering Journal*, *5*(12), 2738–2746. https://doi.org/10.28991/cej-2019-03091445

Tapela, B., & Massingue, F. (2010). *Roadmap for Stakeholder Participation for the Limpopo Watercourse Commission - LIMCOM*.

Tapley, B. D., Watkins, M. M., Flechtner, F., Reigber, C., Bettadpur, S., Rodell, M., Sasgen, I., Famiglietti, J. S., Landerer, F. W., Chambers, D. P., Reager, J. T., Gardner, A. S., Save, H., Ivins, E. R., Swenson, S. C., Boening, C., Dahle, C., Wiese, D. N., Dobslaw, H., … Velicogna, I. (2019). Contributions of GRACE to understanding climate change. In *Nature Climate Change* (Vol. 9, Issue 5, pp. 358–369). Nature Publishing Group. https://doi.org/10.1038/s41558-019-0456-2

The Limpopo Watercourse Commission (LIMCOM). (2003). *Agreement between the Republic of Botswana, the Republic of Mozambique, the Republic of South Africa, and the Republic of Zimbabwe*.

van Wyck, A. E., & Smith, G. E. (2001). *Regions of Floristic Endemism in Southern Africa: A Review with Emphasis on Succulents*. Umdaus Press.

Walker, D., Jovanovic, N., Bugan, R., Abiye, T., du Preez, D., Parkin, G., & Gowing, J. (2018). Alluvial aquifer characterisation and resource assessment of the Molototsi sand river, Limpopo, South Africa. *Journal of Hydrology: Regional Studies*, *19*, 177–192. https://doi.org/10.1016/j.ejrh.2018.09.002

Walker, D., Smigaj, M., & Jovanovic, N. (2019). Ephemeral sand river flow detection using satellite optical remote sensing. *Journal of Arid Environments*, *168*, 17–25. https://doi.org/10.1016/j.jaridenv.2019.05.006

Watkins, M. M., Wiese, D. N., Yuan, D. N., Boening, C., & Landerer, F. W. (2015). Improved methods for observing Earth's time variable mass distribution with GRACE using spherical cap mascons. *Journal of Geophysical Research: Solid Earth*, *120*(4), 2648–2671. https://doi.org/10.1002/2014JB011547

Wiese, D. N., Landerer, F. W., & Watkins, M. M. (2016). Quantifying and reducing leakage errors in the JPL RL05M GRACE mascon solution. *Water Resources Research*, *52*(9), 7490–7502. https://doi.org/10.1002/2016WR019344

Xia, Y., Mitchell, K., Ek, M., Sheffield, J., Cosgrove, B., Wood, E., Luo, L., Alonge, C., Wei, H., Meng, J., Livneh, B., Lettenmaier, D., Koren, V., Duan, Q., Mo, K., Fan, Y., & Mocko, D. (2012). Continental-scale water and energy flux analysis and validation for the North American Land Data Assimilation System project phase 2 (NLDAS-2): 1. Intercomparison and application of model products. *Journal of Geophysical Research Atmospheres*, *117*(3). https://doi.org/10.1029/2011JD016048

Xia, Y., Mocko, D., Huang, M., Li, B., Rodell, M., Mitchell, K. E., Cai, X., & Ek, M. B. (2017). Comparison and assessment of three advanced land surface models in simulating terrestrial water storage components over the United States. *Journal of Hydrometeorology*, *18*(3), 625–649. https://doi.org/10.1175/JHM-D-16-0112.1

Zhang, J., Condon, L. E., Tran, H., & Maxwell, R. M. (2020). *A national topographic dataset for hydrological modeling over contiguous United States*. https://doi.org/10.25739/e1ps-qy48

APPENDIX

Electrical Resistivity Tomography Methods

Electrical resistivity tomography (ERT) is one field method of assessing groundwater resources. The system outputs the subsurface resistivity distribution by making measurements from the ground surface. Our application assumes that resistivity has negligible change perpendicular to the survey line. Measurements are conducted by the application of current through the ground across a series of electrodes and measuring the resultant voltage across different electrodes. From the current and voltage values, an apparent resistivity value is calculated. Ground resistivity is related to various geological parameters such as the mineral content, fluid content, porosity, saturation of water, and dissolved ions. ERT investigations can thus be used to identify subsurface zones with varying electrical properties. The true subsurface resistivity can be determined by performing an inversion process on the apparent resistivity measurements. Once resistivity values are obtained, comparing these values to typical resistivity values of regional subsurface materials can provide information about the geological structure of the subsurface, including types of rock present and location of groundwater.

In this study an ERT profile was carried out on July 30th, 2022, at a location perpendicular to a small, unnamed tributary of the Sand River in the Soutpansberg Mountains, which was the focus of the developed model in section 3.4. The ERT transect was approximately 13 km away from the outlet of the watershed at Waterpoort (Figure 20). The transect was created by laying two 120 m cables in line with each other perpendicular to the tributary. At the center of the transect, the cables were connected to a 48-channel resistivity imaging system (SYSCAL Pro, IRIS Instruments, Orleans, France). The electrodes for this transect were 5 meters apart. The Wenner-Schlumberger array configuration was used (Jamaluddin & Umar, 2018). This

configuration has a constant system of spacing rules for four electrodes, where the current electrodes are on either end, and the potential electrodes are in the middle. The total length of the transect was 230 meters and 46 electrodes were used. The resistivity data inversions were iteratively carried out through the ResIpy windows software (Blanchy et al., 2020). Bad data points having extremely high or extremely low values when compared with surrounding values were removed. The selected inversion process uses the least-square method to determine the true subsurface resistivity distribution.

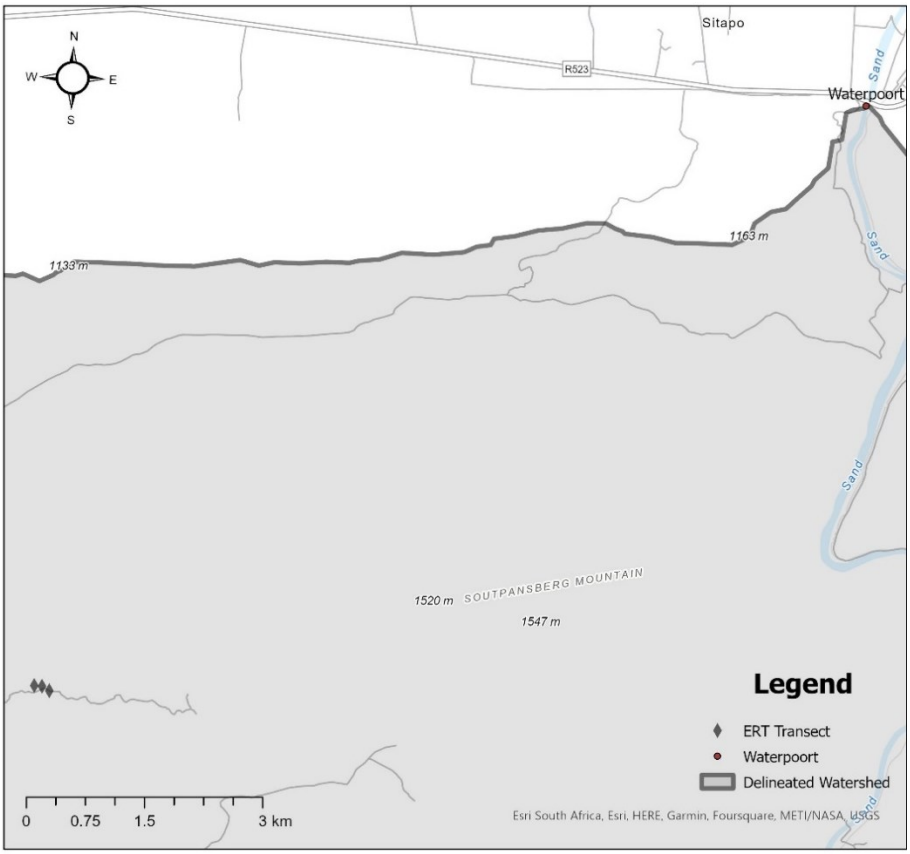

Figure 20. Location of ERT transect in the Soutpansberg Mountains watershed.

Electrical Resistivity Tomography Results

The survey line for the ERT transect was positioned perpendicular to the unnamed tributary of the Sand River catchment. Elevation and distance along the transect is shown (Figure

21). The survey line begins on one side of the tributary and crosses the shortest width of the tributary between 25 and 30 meters. The elevation range for the transect was 1193 meters to 1214 meters. Post-processing results of the apparent resistivity measurements of the transect are shown as the inversion resistivity values (Figure 22). The presence of water corresponds to resistivity values between 10 Ωm and 30 Ωm (Kollert, 1969). Each set of processed results shows the presence of water in the subsurface between 40 and 80 meters along the transect line and between approximately 10 and 40 meters below the surface. These results confirm a groundwater presence and support the findings from the modelled infiltration.

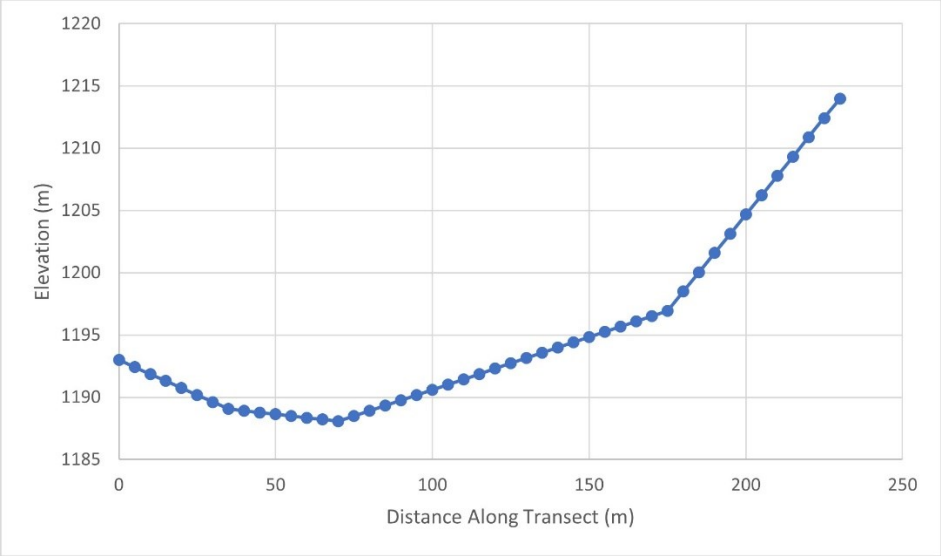

Figure 21. Elevation along ERT transect of the tributary of the Sand River in the Soutpansberg Mountains.

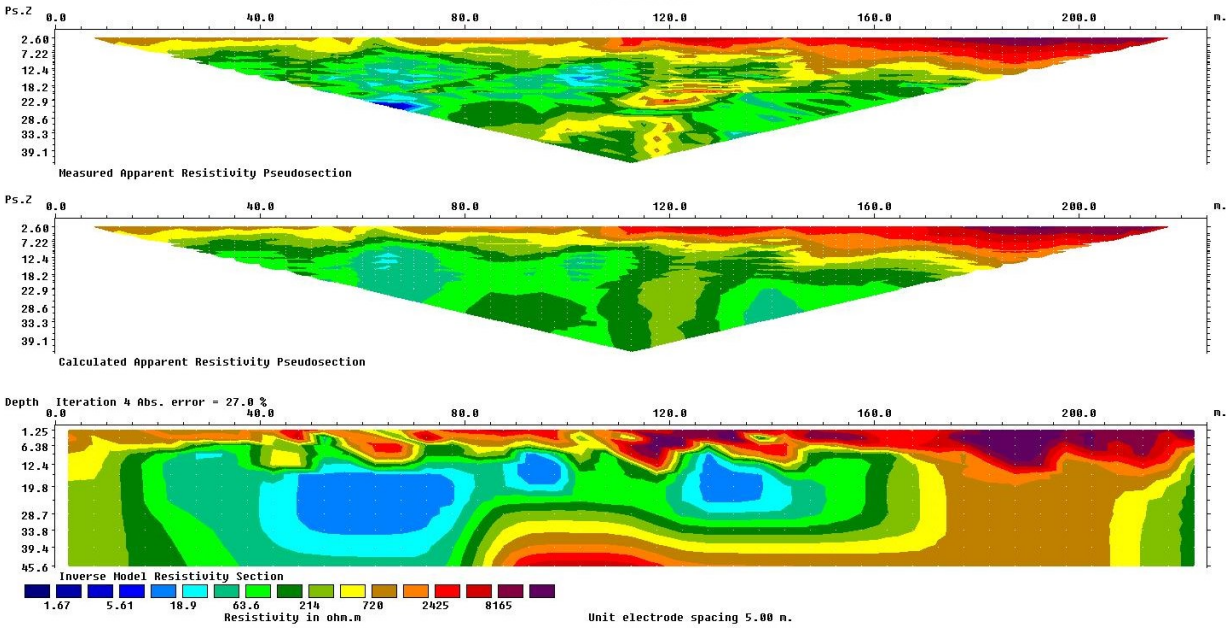

Figure 22. Resistivity results of ERT survey showing measured apparent resistivity, calculated apparent resistivity, and the inversion modelled resistivity of the transect.